[1] Fluorescence: Basic Concepts, Practical Aspects, and Some Anecdotes

By DAVID M. JAMESON, JOHN C. CRONEY, and PIERRE D. J. MOENS

Introduction

The theoretical foundations of fluorescence spectroscopy were established in the first half of the twentieth century by pioneers including Enrique Gaviola, Jean and Francis Perrin (father and son), Peter Pringsheim, Sergei Vavilov, F. Weigert, F. Dushinsky, Alexander Jabłoński, Theodor Förster, and, more recently, Gregorio Weber.[1–7] In the last quarter of the twentieth century, advances in electronics, lasers, computers, and molecular biology have allowed fluorescence methodologies to assume an important role in diverse disciplines including chemistry, cell biology, and the biomedical sciences. This volume of *Methods in Enzymology* covers many of the most exciting new developments in fluorescence spectroscopy—developments and techniques that presently define the state of the art. In this article, however, we wish to remind readers of the origins of several important aspects of fluorescence spectroscopy. We also wish to discuss some practical aspects of fluorescence determinations which are sometimes forgotten as those new to these methods often focus on learning the software associated with commercial instrumentation. Much of the modern "point-and-click" software approach allows the novice to immediately apply fluorescence methods to their particular research problems, taking advantage of the highly sophisticated instrumentation and probe chemistries that are now readily available. However, kits and user-friendly software should not dissuade beginners from learning the fundamentals of fluorescence methodologies and instrumentation. Such knowledge not only allows avoidance of potential pitfalls, recognition of artifacts, and fuller appreciation of the applicability of fluorescence techniques, it also makes the research more interesting and fun! We should also point out that although fluorescence measurements are usually carried out with sophisticated and expensive instrumentation,

[1] G. Weber, *Methods Enzymol.* **278,** 1 (1997).
[2] B. Nickel, *EPA Newslett.* **58,** 9 (1996).
[3] B. Nickel, *EPA Newslett.* **61,** 27 (1997).
[4] B. Nickel, *EPA Newslett.* **64,** 19 (1998).
[5] M. N. Berberan-Santos, *in* "New Trends in Fluorescence Spectroscopy" (B. Valeur and J.-C. Brochon, eds.), p. 7. Springer-Verlag, Heidelberg, Germany, 2001.
[6] D. M. Jameson, *in* "New Trends in Fluorescence Spectroscopy" (B. Valeur and J.-C. Brochon, eds.), p. 35. Springer-Verlag, Heidelberg, Germany, 2001.
[7] B. Valeur, "Molecular Fluorescence: Principles and Applications." Wiley-VCH, Weinheim, Germany, 2002.

0076-6879/03 $35.00

many of the basic principles of fluorescence can be appreciated and demonstrated with a simple ultraviolet (UV) hand lamp.[8]

Virtually all fluorescence data required for any research project will fall into one of the following categories: (1) the fluorescence emission spectrum, (2) the excitation spectrum of the fluorescence, (3) the quantum yield, (4) the fluorescence lifetime, or (5) the polarization (anisotropy) of the emission.

In this article, we examine each of these categories and briefly discuss historical developments, underlying concepts, and practical considerations. We preface these discussions with an overview of the most salient aspects of three essential pieces of fluorescence hardware, namely, light sources, monochromators, and detectors (specifically photomultipliers). Finally, we discuss the phenomenon of fluorescence resonance energy transfer (FRET)—a topic in vogue presently. Our discussion of FRET, however, does not follow the path already trodden by numerous reviews but instead focuses sharply, and in some detail, on energy transfer between like molecules, that is, homo-FRET.

Before delving into our discussion of the theory and practice of fluorescence measurements, we should briefly mention the realm of potential fluorophores. Fluorescence probes can be broadly placed into two categories: intrinsic probes and extrinsic probes. By intrinsic we mean any naturally occurring molecule which exhibits sufficient fluorescence to be of practical utility. Examples include the aromatic amino acids, especially tryptophan and tyrosine, NADH, FAD, FMN, some porphyrins, some fatty acids and lipids, some modified nucleic acids (such as the Wye base in some tRNAs), pyridoxal phosphate, chlorophylls, pteridines, and some others. By extrinsic we mean probes that can be introduced into the target system to form a complex, either noncovalent or covalent. Up until the late 1970s, the choice of commercially available probes was limited; typically, researchers [such as one of the authors (D.M.J.) of this article] had to design and synthesize fluorophores for particular types of studies. The choice of fluorophore was dictated by the properties of the instruments [light sources and photomultiplier tube (PMT) sensitivities] as well as by the lifetimes and spectral properties required. The first probe made for physicochemical studies of proteins was dimethylaminonaphthalene sulfonyl chloride (dansyl choride), synthesized by G. Weber and designed to be conjugated to proteins and used for fluorescence polarization measurements.[9,10] In the last two decades, however, the availability of fluorescence probes, principally by the company Molecular Probes (Eugene, OR; www.probes.com), has expanded incredibly. Literally thousands of probes are now available. Examples of common noncovalent probes are 8-anilino-1-naphthalene sulfonate (ANS), 1,6-diphenyl-1,3,5-hexatriene (DPH), 2-dimethylamino-6-lauroylnaphthalene (Laurdan), ethidium bromide, Hoechst

[8] J. C. Croney, D. M. Jameson, and R. P. Learmonth, *Biochem. Mol. Biol. Ed.* **29,** 60 (2001).
[9] G. Weber, *Biochem. J.* **51,** 145 (1952).
[10] G. Weber, *Biochem. J.* **51,** 155 (1952).

dyes, 4′,6-diamidino-2-phenylindole (DAPI), to name but a few, while covalent probes functionalized with reactive groups such as sulfonyl choride, isothiocyanate, succinimidyl ester, iodoacetamide, maleimide, hydrazine derivatives, and others are available to target a wide variety of biomolecules. In addition to probes specifically designed to target biomolecules for solution studies, a wide range of probes exist which are specialized for fluorescence microscopy studies on living cells.

Basic Instrumentation

A typical modern spectrofluorimeter is shown in Fig. 1 (adapted with permission from ISS, Inc.), which illustrates the principal components and the general layout (we have adopted the nomenclature of "fluorimeter" for steady-state instrumentation and "fluorometer" for lifetime instrumentation, a custom that originated

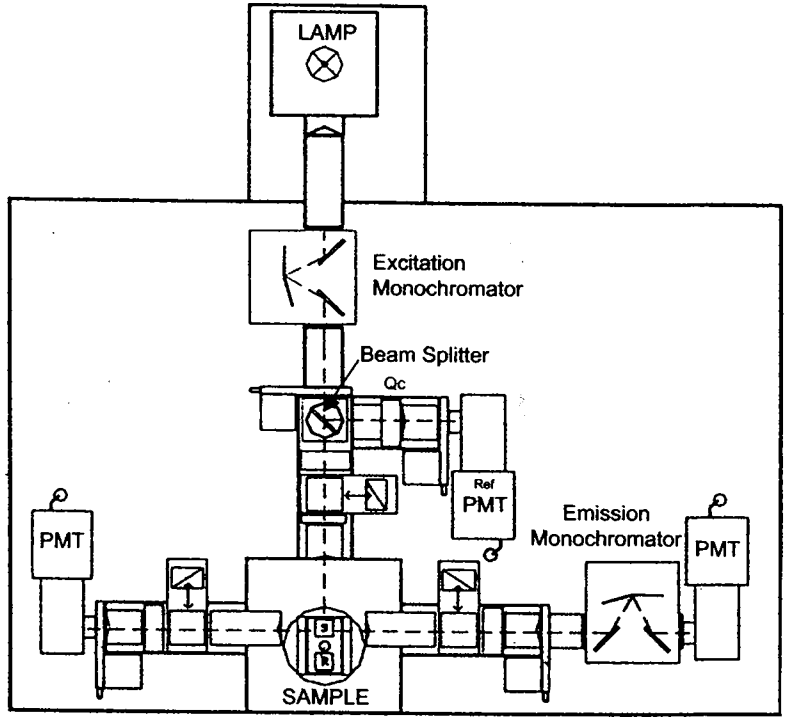

FIG. 1. Schematic diagram of a spectrofluorimeter (revised with permission from commercial literature from ISS, Champaign, IL). The principal components include the xenon arc lamp, the excitation and emission monochromators, a quartz beam splitter, a quantum counting solution (Qc), three photomultiplier tubes (PMT), and excitation (P_{ex}) and emission (P_{em}) calcite prism polarizers.

with Gaviola,[11] who termed his lifetime instrument a fluorometer). Clearly the starting point for any fluorescence observation is the light source. Fortunately, we no longer need to rely on sunlight as the principal excitation source for fluorescence. A comprehensive discussion of the development of light sources is beyond the scope of this article, but a good overview of a wide range of light sources (and many other relevant topics such as filters, monochromators, and photodetectors) can be found in the book by Moore *et al.*[12] We shall restrict ourselves to consideration of the light sources most commonly employed in commercial fluorescence instrumentation, namely the xenon arc lamp, the xenon–mercury arc lamp, lasers, light-emitting diodes (LEDs), and laser diodes. We should note that the most common light sources used in absorption spectrophotometry, deuterium and tungsten lamps, are rarely used in fluorescence since they are relatively weak photon sources.

For our present discussion the most relevant aspect of light sources is the useful wavelength range. From this point of view the xenon arc lamp is by far the most common light source in commercial instruments since it produces usable light from the ultraviolet to the infrared. This range is adequate for most fluorescence studies of biological samples since such studies are usually limited by the absorption characteristics of water at either end of this spectral range, and by photodamage in the deep ultraviolet. An example of the light distribution from a xenon arc lamp, from 220 to 590 nm, is shown in Fig. 2 (this spectrum is convoluted by the characteristics of the excitation monochromator and quartz beam splitter—topics which will be discussed later). Although the spectral range shown is relatively narrow, we should note that xenon arc lamps provide significant illumination out to around 2000 nm. Clearly the intensity of this light source depends dramatically on the wavelength—a fact which has a significant impact on the excitation spectrum, as discussed later. The xenon–mercury arc has the characteristics of the xenon arc source but is dominated by very prominent lines due to the mercury transitions. The more prominent mercury lines are near 254, 297, 302, 313, 365, 405, 436, 546, and 578 nm.[13] Much of the early work on proteins carried out in the former Soviet Union utilized 296.7 nm as the excitation wavelength since mercury lamps were a common light source at that time; the choice of this wavelength was appropriate since tyrosine absorption is negligible above 295 nm and hence tryptophan residues could be preferentially excited.

The use of lasers in fluorescence has primarily been restricted to time-resolved instrumentation, due to the intensity and spatial characteristics of laser sources [with the notable exception of fluorescence-activated cell sorters (FACS)]. Of course, laser sources have distinct emission lines characteristic of the atomic

[11] E. Gaviola, *Z. Physik.* **35,** 748 (1926).

[12] J. H. Moore, C. C. Davis, and M. A. Coplan, "Building Scientific Apparatus: A Practial Guide to Design and Construction." Addison-Wesley, Reading, MA, 1983.

[13] C. J. Sansonetti, M. L. Salit, and J. Reader, *Appl. Optics* **35,** 74 (1996).

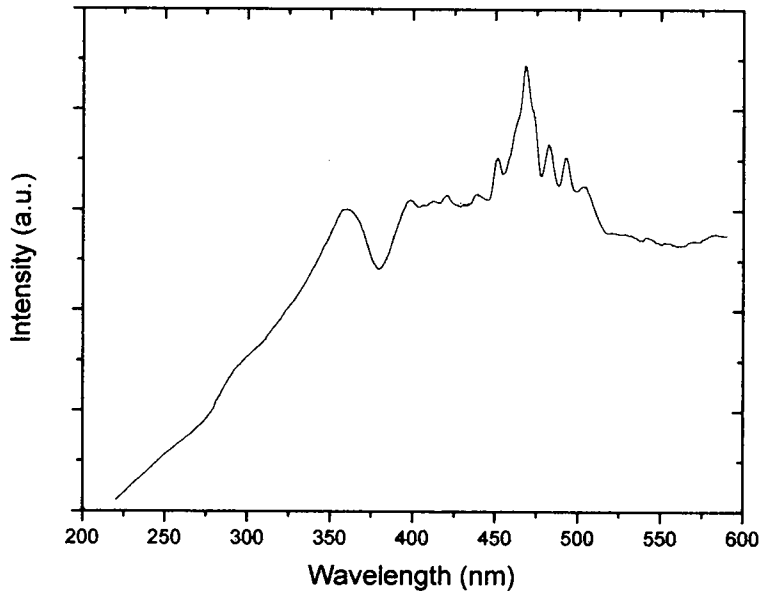

FIG. 2. Spectral distribution from a xenon arc lamp: obtained using the ISS PC1 spectrofluorimeter shown in Fig. 1.

processes involved. The most commonly used lasers in modern biological fluorescence spectroscopy are the argon ion laser, the helium–cadmium laser, the neodymium:yttrium–aluminum–garnet (Nd:YAG) laser and, more recently, the titanium–sapphire laser. The most commonly used argon ion laser lines are near 488 and 514 nm. Large-frame, high-power argon ion lasers [e.g., the Spectra-Physics (Mountain View, CA) model 2045 laser in the authors' laboratory] produce lines in the deep UV at 275 nm and between 300 and 305 nm as well as the mid-UV near 334, 351, and 364 nm and in the visible near 457, 476, 488, 497, 501, 514, and 528 nm. Helium–cadmium lasers produce lines near 325 and 442 nm. Nd:YAG lasers emit at 1064 nm and are typically doubled or quadrupled to 532 and 266 nm, respectively (frequency-doubled Nd:YAG lasers are now readily available as green-emitting laser pointers). Often, the doubled Nd:YAG output at 532 nm is used to pump a dye laser (typically a rhodamine-based dye) whose output in a range around 600 nm can then be doubled to produce UV light over a range around 300 nm. The titanium–sapphire laser, which emits over a range of about 700–1000 nm, is presently the light source of choice for multiphoton excitation. A relevant characteristic of laser sources is the time profile of their output; for example, typical argon ion or helium–cadmium lasers are operated as continuous sources (termed CW; intensity essentially time invariant) whereas Nd:YAG and titanium–sapphire lasers are usually operated as pulsed sources.

LEDs are becoming more popular since the list of available wavelengths is growing and, more importantly, extending deeper into the UV. At the time of this writing, LED sources down to 370 nm are available commercially. LEDs are much less intense than lasers (and not collimated) but have the advantages that they are relatively inexpensive, low-power, solid-state devices that generate little heat and which provide usable intensities over a narrow (but not discrete) spectral range. Their energy output can also be directly modulated, which suggests time-resolved applications (discussed below). Another solid-state device, the laser diode, provides monochromatic radiation; near-UV laser diodes have become available which are much more intense than LEDs but which—at the time of this article—only extend down to about 400 nm.

If the excitation light source is not at a discrete wavelength, that is, a laser or laser diode, then a device capable of wavelength selectivity is required, typically either an optical filter or a monochromator. For excitation purposes, the most useful optical filter is usually an interference-type filter, which typically can isolate wavelengths with a resolution of a few nanometers. The figure of merit for these types of filters is their full width at half-maximum (FWHM). For example, an interference filter centered at 400 nm with an FWHM of 5 nm transmits 50% of the intensity at 395 and 405 nm that it transmits at 400 nm. Such filters are not always very efficient, especially as the wavelength decreases. For example, the peak light transmission efficiency of a typical UV interference filter may be ~20% compared to ~70 to 80% for an interference filter centered in the visible wavelength region. Other types of filters used in fluorescence studies will be discussed when the emission side of the fluorimeter is considered.

Monochromators are the most common and versatile devices used to isolate specific wavelengths of light from broad-band sources such as xenon arc lamps. Monochromators operate by dispersing the incident light—most people are very aware of the light-dispersing qualities of a prism (we note that most people have observed the excellent light dispersion qualities of raindrops, which result in rainbows, but far fewer notice that the weaker of the double rainbows, which can occur under particularly sunny conditions, has the order of the colors reversed due to the additional raindrop-interior reflection). The spectral region selected by a monochromator depends on the design of the monochromator and, ultimately, on the physical size of the monochromator slits; the key consideration here is the dispersion of the monochromator, which allows conversion of the physical width of a slit (e.g., in millimeters) to the FWHM of the spectral region passed. For example, the monochromators in the instrument shown in Fig. 1 utilize fixed slits (as opposed to infinitely variable slits) and have dispersions of 8 nm per millimeter. Slits ranging from 0.025 to 4 mm are commonly available, which thus supply spectral resolutions ranging from 0.2 to 32 nm. Different monochromators, of course, have different dispersion factors but the common feature is that the smaller the slit, the higher will be the spectral resolution. This resolution comes with a cost, namely, a reduction in the light intensity: a 2-fold reduction in each slit width

(entrance or exit) results in an approximate 4-fold decrease in light intensity. In commercial spectrofluorimeters, prism-based monochromators are not commonly used, one reason being that a linear scan of the prism assembly will not result in a linear dispersion of wavelengths. For many years, commercially available monochromators [such as those from Bausch & Lomb (Rochester, NY) or Thermo Jarrell Ash (Franklin, MA)] used planar ruled diffraction gratings as the dispersive element. These devices worked well but exhibited parasitic light levels due to imperfections in the ruling process, which could seriously hamper measurements of turbid samples. This source of stray light was dramatically reduced when concave holographic gratings became available. These types of diffraction gratings are made using interference patterns generated onto photoresist substrates using laser sources. One of the first widespread commercial uses of holographic gratings in spectrofluorimeters was by SLM in the early 1970s [the gratings themselves were from Jobin Yvon (Edison, NJ)]. Regardless of the type of grating utilized, the efficiency with which a monochromator transmits light will show both wavelength and polarization dependence (discussed below).

After the excitation wavelength is isolated it is sometimes passed through a polarizing device to select one plane of polarization (polarization is discussed in more detail below). A variety of devices, both naturally occurring and man-made, have been used to polarize light. The Vikings, in fact, used a "sunstone" to observe the location of the sun on foggy or overcast days (magnetic compasses were unreliable at higher latitudes)—days that lasted a long time at the high northern latitudes! This stone is now thought to have been composed of the mineral cordierite, a natural polarizing material. By taking advantage of the fact (even if they did not know the reasons behind it) that scattered sunlight was highly polarized whereas light coming along the direction of the sun was not, Vikings could observe the distribution of the sky's brightness through the sunstone and localize the position of the sun and, if the time of day were known, the compass directions. Nowadays, the most common polarizers are either dichroic devices, which operate by effectively absorbing one plane of polarization (e.g., Polaroid type-H sheets based on stretched polyvinyl alcohol impregnated with iodine, invented in 1926 by E. H. Land while he was a freshman at Harvard), or double-refracting calcite ($CaCO_3$) crystal polarizers (discovered independently by Erasmus Bartholin and Christiaan Huygens in the seventeenth century), which differentially disperse the two planes of polarization (examples of this class of polarizers are Nicol polarizers, Wollaston prisms, and Glan-type polarizers such as the Glan–Foucault, Glan–Thompson, and Glan–Taylor polarizers). [Typically film polarizers are inexpensive but do not transmit efficiently in the ultraviolet. (Quiz: The interested reader should work out which direction of polarized light polarizing sunglasses pass; Hint—glare or light reflected from surfaces is largely polarized in a horizontal direction).] Calcite prism polarizers, on the other hand, transmit well into the ultraviolet (<240 nm) but are expensive (in the range of U.S. $1000) and have small apertures and angular acceptance tolerances, which means that incident light

cannot be tightly focused (a comparison of the wavelength-dependent polarizing efficiencies of several types of polarizing devices is given in Jameson *et al.*[14]

In our typical fluorimeter, the exciting light impinges on the sample and the emission is viewed at right angles to the direction of excitation (Fig. 1). This 90° observation angle is primarily intended to reduce the extent of exciting light that passes to the detection side. Only when samples are relatively turbid, for example in the case of lipid suspensions or membrane samples, will significant levels of exciting light be scattered and potentially reach the photodetector (since optical filters and monochromators are not perfect). We should also note that the focal lengths of the lenses just before and after the sample have a small influence on the measured polarization. Specifically, the larger the numerical aperture of the lenses focusing the excitation and collecting the emitted light (i.e., the shorter the focal length and hence the larger the cone of collected light), the lower the measured polarization compared to the true polarization.[15] This effect is most serious in microscope optics, having only a small influence on measurements taken with normal spectrofluorimeters. A typical instrument such as that shown in Fig. 1 may yield a polarization lower by only a few percent from the true value. After excitation by the polarized light, the emitted light can (if desired) also be passed through a polarizing device and the spectral region of interest can be isolated by an optical filter or a second monochromator. The usual filters used in the emission side are either bandpass filters (which transmit a broader spectral region than interference filters; FWHMs can be several tens of nanometers or greater) or cut-on filters. This latter filter is often referred to as a cut-off filter, depending on the viewpoint of whether the transmission commences sharply at a given wavelength (cuts on) or, equivalently, if the optical density decreases sharply at that wavelength (cuts off). Regardless, the operational principle of these types of filters, which are also known as longpass filters, is that they can be used to block any excitation light scattered toward the emission direction and then collect a large percentage of the total emission. Web sites that contain transmission data for many types of filters include www.mellesgriot.com and www.corion.com. A useful handbook containing information about filters for fluorescence microscopy can be found at www.chroma.com.

Most modern instruments use photomultiplier tubes (PMTs) for detection and quantification of the emitted light. These devices are, of course, based on the photoelectric effect, that is, the ejection of electrons from metallic surfaces as a consequence of incident light. The theory for this effect was developed by Albert Einstein, who received the Nobel Prize for this work and not for his more famous theory of relativity. The original phototubes were based on a simple arrangement to collect the emitted photoelectrons and produce an electric current, which could then be quantified. These early devices were not much of an

[14] D. M. Jameson, G. Weber, R. D. Spencer, and G. Mitchell, *Rev. Sci. Instrum.* **49,** 510 (1978).
[15] G. Weber, *J. Opt. Soc. Am.* **46,** 962 (1956).

improvement over the human eye, although they did offer the considerable advantage of protecting the observer from the deleterious effect of UV or infrared (IR) radiation on the visual system. PMT devices were soon developed, however, that had multiple plates after the photosensitive cathode, called dynodes, held at progressively more positive voltages, which acted as secondary electron-emitting surfaces and which would eject several electrons for each incident electron and hence multiply the effect manyfold (practical gains above 10^9 anode electrons per photoelectron can be achieved for short light pulses although continuous gains of about 10^7 are typical, due to thermal loading in the final dynodes). In the last few decades, significant progress had been made in the commercialization of PMTs with "extended red response," which essentially means PMTs that can efficiently detect light out to beyond 800 nm. One of the first widely used PMTs in this category was the Hamamatsu (Bridgewater, NJ) R928 (a side-on, nine-stage PMT with a multialkali photocathode rated from 185 to 900 nm). One of the authors (D.M.J.) vividly remembers being handed one long ago by Gregorio Weber, with instructions to "try it out!" At that time it seemed miraculous because it so greatly minimized the correction factors (discussed below) needed to acquire true molecular spectra extending above 600 nm. For detailed information about a variety of PMTs and other types of detectors, the reader can refer to http://usa.hamamatsu.com.

Emission Spectra

Using complementary filters, George Gabriel Stokes realized in 1852[16] that the fluorescence phenomenon, which he originally termed "dispersive reflexion" but, in a subsequent article renamed "fluorescence," resulted in the emission of light at longer wavelengths than the absorbed light, and his name is still used to describe this wavelength shift (for an illuminating account of the origins of the terms fluorescence, phosphorescence, and luminescence see Valeur[7]). Early observations on fluorescence relied on various types of filters (usually chemical solutions, sometimes even wine!) to block the exciting light (interestingly, C. V. Raman, in his pioneering work on the effect that now bears his name, had to use filters to block out fluorescence). Modern filters are usually made of sophisticated glasses or plastics and include cut-on, cut-off, bandpass, and interference type filters (discussed above). It is interesting to note that most of the important original observations on fluorescence were made almost exclusively by visual methods since reliable and sensitive photomultipliers came into popular use only after World War II.[17,18]

[16] G. G. Stokes, *Philos. Trans.* **142,** 463 (1852).

[17] G. Weber, *in* "Time-Resolved Fluorescence Spectroscopy in Biochemistry and Biology" (R. B. Cundall and R. E. Dale, eds.), Vol. 69, p. 1. Plenum Press, New York, 1983.

[18] G. Weber, *in* "Fluorescent Biomolecules" (D. M. Jameson and G. D. Reinhart, eds.), p. 343. Plenum Press, New York, 1989.

Consequently, many of the pioneers in this field, such as Gregorio Weber, suffered from acute eye ailments in later life.[6]

In the middle of the twentieth century commercial fluorescence instrumentation began to appear. The earliest commercial instruments were essentially attachments for spectrophotometers, such as the Beckman (Fullerton, CA) DU spectrophotometer[19]; this attachment allowed the emitted light (excited by the mercury vapor source through a filter) to be reflected into the monochromator of the spectrophotometer. The first commercial spectrofluorimeters with monochromators for both excitation and emission were inspired by the work of Bowman *et al.*,[20] and were produced by AMINCO-Bowman and Farrand. These early instruments allowed biologists to use fluorescence to develop clinically relevant assays for a wide variety of biological molecules.[19] Among the first emission spectra with direct significance for protein chemists were those of the aromatic amino acids, published in 1957 by Teale and Weber.[21]

Early examination of a large number of emission spectra resulted in the formulation of certain general rules.

1. *In a pure substance existing in solution in a unique form, the fluorescence spectrum is invariant, remaining the same independent of the excitation wavelength.* In fact, if the fluorescence spectrum changes as the excitation wavelength varies, one may usually conclude that there are more than one emitting species present (exceptions may be due to dipolar relaxation or other excited state effects such as deprotonation, which will not be discussed here).

2. *The fluorescence spectrum lies at longer wavelengths than the absorption.* If the absorption maximum of the band of least frequency is at wavelength λ_{abs} and the maximum of the fluorescence emission is at λ_{fl} it is always found that $\lambda_{abs} < \lambda_{fl}$ or $\nu_{abs} > \nu_{fl}$, where ν corresponds to c/λ.

3. *The fluorescence spectrum is, to a good approximation, a mirror image of the absorption band of least frequency.* The wavelength of reflection is found midway between ν_{abs} and ν_{fl} and corresponds to the energy of the pure electronic transition ($0 \rightarrow 0'$).

These general observations follow from consideration of the Perrin–Jabłoński diagram shown in Fig. 3 (we use this term to recognize the fact, as pointed out by Nickel,[2] that F. Perrin actually utilized energy level diagrams to describe fluorescence phenomena before Jabłoński; the most recent text on fluorescence by B. Valeur[7] also adopts this nomenclature). Specifically, although the fluorophore may be excited into different singlet state energy levels (e.g., S_1, S_2, etc.) rapid

[19] S. Udenfriend, "Fluorescence Assay in Biology and Medicine." Academic Press, New York, 1962.
[20] R. L. Bowman, P. A. Caufield, and S. Udenfriend, *Science* **122,** 32 (1955).
[21] F. W. J. Teale and G. Weber, *Biochem. J.* **53,** 476 (1957).

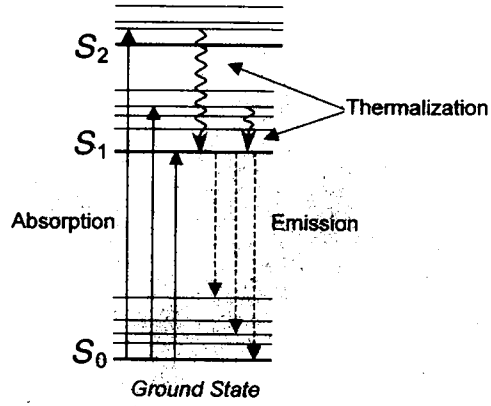

FIG. 3. Perrin–Jabłoński diagram. S_0 is the ground state, whereas S_1 and S_2 are electronically excited states. The time scales of the absorption, thermalization, and emission processes are typically in the range of $\sim 10^{-15}$, $\sim 10^{-12}$, and $\sim 10^{-9}$ sec, respectively.

thermalization invariably occurs and emission takes place from the lowest vibrational level of the first excited electronic state (S_1). Only in a few rare cases, such as azulene, does emission occur from the S_2 level (see, e.g., Liu[22]). This fact accounts for the independence of the emission spectrum from the excitation wavelength. The fact that ground state fluorophores, at room temperature, are predominantly in the lowest vibrational level of the ground electronic state (as required from the Boltzmann distribution law) accounts for the Stokes shift. Finally, the fact that the spacings of the energy levels in the vibrational manifolds of the ground state and first excited electronic states are usually similar accounts for the fact that the emission and absorption spectra (plotted in energy units such as reciprocal wavenumbers) are approximately mirror images (although emission spectra are usually plotted in terms of wavelengths, most modern software allows for facile conversion and display in terms of wavenumbers).

Virtually all modern spectrofluorimeters use right-angle geometry, that is, the direction of observation of the emitted light is 90° to that of the excitation. As mentioned above, this geometry was chosen to allow for a more complete elimination of exciting light from the observed signal. In other words, the unabsorbed excitation light will continue through the cuvette and be absorbed by the blackened sample compartment. This right-angle observation geometry is the reason, of course, that fluorescence cuvettes, as opposed to absorption cuvettes, have all four sides polished (occasionally novices are observed using absorption cuvettes in spectrofluorimeters, which usually leads to disappointing results!). While on the topic

[22] R. S. H. Liu, *J. Chem. Ed.* **79**, 183 (2002).

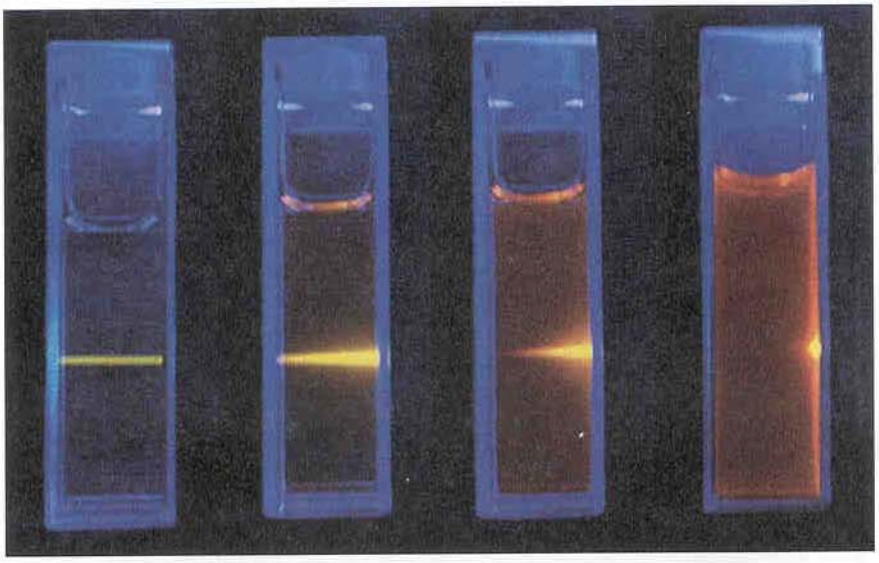

FIG. 4. Rhodamine B in ethanol excited by Nd : YAG laser pointer device (in each case, the light is passing through the cuvette from the right to the left). Optical densities are 0.04, 1.0, 3.0, and >30, from left to right, respectively.

of cuvettes, we should also note that quartz (or fused silica) cuvettes are normally used because they transmit down to the deep UV, and if glass or plastic cuvettes are being used one must be aware of their wavelength cutoff points. This right-angle geometry also immediately demands consideration of the effect of sample optical density on the observed signal. This effect is illustrated in Fig. 4, which depicts excitation light impinging on four samples of rhodamine B in ethanol, with optical densities (at 532 nm, the wavelength from the green laser pointer utilized to excite the fluorescence) ranging from 0.04 to greater than 30. It is readily apparent that the excitation light traverses, virtually undiminished in intensity, the sample with the low (0.04) optical density, whereas it is significantly absorbed by sample with an optical density equal to 1, largely absorbed by sample with optical density equal to 3, and completely absorbed by the most concentrated sample. Since the emission optics are typically focused on the center of the cuvette, one can easily see that the observed signal will suffer as a consequence of absorption of the exciting light by the initial layers of the solution. In such a case, increasing the concentration of the sample in an effort to increase the signal will lead to even less detected fluorescence. One simple way to mitigate this problem—if a high concentration must be utilized, for example, to study weak binding equilibria, or if the quantum yield is low—is to use a cuvette with a reduced pathlength. A T-shaped cuvette, for example, with one long and one short dimension, can be used with the short direction oriented to receive the excitation. Front-face observation, either using

a specially designed sample compartment or a triangular cuvette, may also be used to circumvent inner filter effects (see, e.g., Hirsch[23]). Web sites describing a wide variety of cuvettes include www.optiglass.com and www.nsgpci.com. If the Stokes shift of the fluorophore is small, it may also be necessary to worry about absorption of the emitted light by the solution along the emission path. Various mathematical methods to correct the observed fluorescence intensity for these so-called "inner filter" effects have been described.[7,24] Such inner filter effects are less important for either polarization or lifetime measurements because, in these cases, the property being measured does not depend (up to a point) on the absorption by the solution.

In a typical emission spectrum, the excitation wavelength is fixed and the fluorescence intensity versus wavelength is obtained (we note that some analytical techniques actually use synchronous scanning, wherein both excitation and emission wavelength are scanned simultaneously; however, this specialized method is not discussed further). Typically, the intensity axis of spectra is reported in "arbitrary units." This nomenclature recognizes the fact that the observed intensity depends not only on the concentration of the fluorophore and on molecular factors such as the extinction coefficient and quantum yield of the fluorophore, but also on instrumental factors such as slit widths, PMT voltage, and amplifier gains (photon-counting methods are discussed below), considerations that arise because the normal spectrofluorimeter is not a double-beam instrument like a typical spectrophotometer. Fluorescence spectra recorded in this manner are "technical" or "uncorrected" emission spectra. Uncorrected spectra do not take into account the wavelength-dependent response of the emission optics (principally the monochromator) and the photodetector (most commonly a photomultiplier tube). Up until the mid-1970s or so, most of the PMTs (such as the popular EMI 6256S) used in commercial and even homebuilt instruments had responses that fell off dramatically at wavelengths above 600 nm. Consequently, instrument correction factors (discussed in more detail below) for compounds such as porphyrins and rhodamines (with emission maxima above 600 nm) or even fluorescein (with an emission maximum near 520 nm) were not insignificant. In the late-1970s, however, PMTs with extended red responses (such as the Hamamatsu 928 mentioned above) became almost standard and made emission correction factors much less dramatic. At about the same time holographic diffraction gratings began to appear in commercial instruments—such as the SLM 8000—which featured significantly less parasitic or stray light than the conventionally ruled gratings. Even these modern monochromators, however, exhibit nonideal behavior, which can seriously confuse the novice. One of the more dramatic effects is the so-called Wood's anomaly. In 1902, R. W. Wood observed that diffraction gratings exhibited some anomalous transmission characteristics in narrow spectral regions. These anomalies, known

[23] R. E. Hirsch, *Methods Enzymol.* **232,** 231 (1994).

[24] J. R. Lakowicz, "Principles of Fluorescence Spectroscopy." Kluwer Academic, New York, 1999.

as "Wood's anomalies," are highly dependent on the polarization of the incident light, being almost entirely polarized perpendicular to the rulings of the grating. They occur in diffraction gratings when a diffracted order becomes tangent to the plane of the grating and are believed to result from a resonant interaction of the incident light with surface plasmons, which are electronic excitations confined to the metal surface.[25] The Wood's anomalies in the monochromators used in the SLM 8000 were discussed in a Ph.D. thesis[26] and an earlier review.[27] (The Wood's anomaly near 380 nm in these monochromators gave a characteristic shoulder in the uncorrected spectrum of intrinsic protein fluorescence, which made it easy to identify the instrument used to obtain the spectrum; in fact, the true "connoisseur" of fluorescence should be able to identify the fluorimeter used from observation of the Wood's anomalies in spectra.) Figure 5 shows scans of a tungsten lamp (in a quartz bulb), which illustrates the Wood's anomalies in an SLM 8000 spectrofluorimeter. The four scans shown correspond to the case of no emission polarizer (Fig. 5A), an emission polarizer oriented parallel to the laboratory axis (Fig. 5B), an emission polarizer oriented perpendicular to the laboratory axis (Fig. 5C), and scan B divided by scan C (Fig. 5D). These scans demonstrate that the Wood's anomalies are located near 380 and 620 nm and, moreover, that they occur only in the perpendicular component. [*Note:* On some instruments, such as the Cary Eclipse (Varian, Palo Alto, CA), the monochromators are mounted with a 90° rotation to render the slit image horizontal, and the resulting Wood's anomalies appear in the parallel component.] Scan D in Fig. 5 furthermore illustrates the fact that the response of the monochromator has a general dependence on the polarization of the observed light.

These considerations bring us to a discussion of emission correction factors. The wavelength and polarization response of the components of any given spectrofluorimeter can be taken into account by generating correction factors specific for that instrument. The correction factors for the emission monochromator, for instance, can be obtained by using a standard lamp. For example, the standard lamp used in D.M.J's thesis[26] was a 45-W halogen–tungsten coiled-coil filament lamp, in a quartz envelope; the spectral irradiance of this lamp, at a distance of 50 cm when the lamp was operated at 6.50 amperes current, was determined by the National Bureau of Standards (the precise current was required because it determined the filament temperature and hence the blackbody radiation spectrum). Thus this lamp was mounted such that light would reach the sample compartment and be reflected from a freshly coated MgO surface (the reflectivity of which was known as a function of wavelength), and one then simply recorded the spectrum.

[25] P. Murdin, *ING La Palma Technical Note* **76,** 1990.

[26] D. M. Jameson, *in* "Biochemistry." University of Illinois, Champaign-Urbana, IL, 1978.

[27] D. M. Jameson, *in* "Fluorescein Hapten: An Immunological Probe" (E. Voss, ed.), p. 23. CRC Press, Boca Raton, FL, 1984.

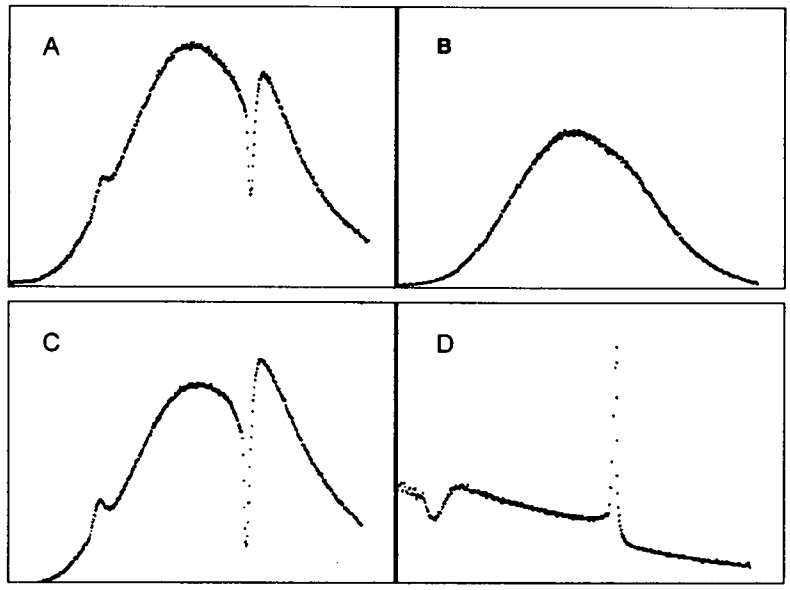

FIG. 5. Scans of a standard tungsten lamp showing Wood's anomalies in an SLM monochromator. Scans A–C are from 251 to 800 nm; scan D is from 351 to 800 nm. Scan A, No polarizer; scan B, parallel emission polarizer; scan C, perpendicular emission polarizer; scan D, ratio of scan B to scan A. Adapted from D. M. Jameson, *in* "Biochemistry." University of Illinois, Champaign-Urbana, IL, 1978.

Comparison of this spectrum with the known spectral irradiance yielded the correction factors. This approach is essentially used by most instrument manufacturers, who now typically supply customers with the appropriate correction factors, usually in a software file. Given our previous discussion of monochromator effects, one can appreciate that the correction factors for parallel polarized light will differ from that for perpendicularly polarized light, as shown in Fig. 6A. To obtain a corrected spectrum for a sample, then one can obtain the technical or uncorrected spectrum through a parallel polarizer and then apply the parallel (vertical) correction factors, as shown in Fig. 6C (technical emission spectra obtained without any polarizer and through a parallel polarizer are shown in Fig. 6B and C, respectively).

Before one applies instrument correction factors, however, one may first have to correct the spectrum for solvent background. Usually this step is not required if the fluorophore has a decent quantum yield and is present at reasonable concentrations, and if a minimum of care was used in preparation of the buffer or solvent. However, if the sample is dilute or the fluorophore is highly quenched then care must be taken, especially regarding the infamous Raman peak. Even though the molar absorptivity due to the O–H stretching mode—which occurs near 3400 cm^{-1}—is weak, the fact that water is 55 *M* means that a measurable quasi-elastic scatter peak can be seen in most fluorimeters (in fact, the ability to resolve Raman

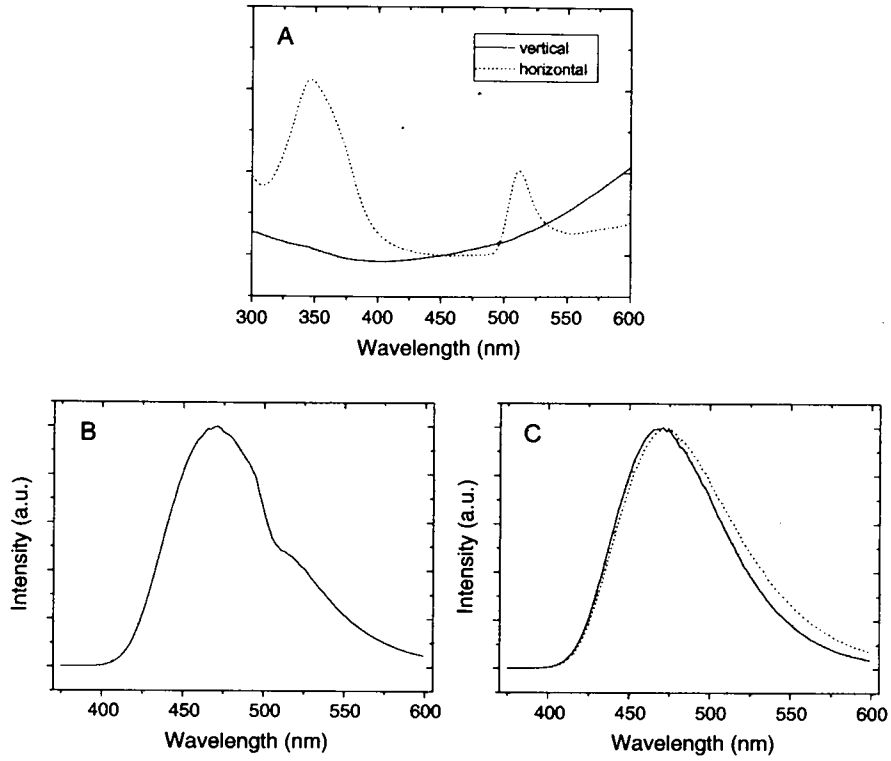

FIG. 6. (A) Emission correction factors for the ISS PC1; parallel (vertical) polarizer factors, solid line; perpendicular (horizontal) polarizer, dotted line. (B) Uncorrected (technical) spectrum for ANS in ethanol, no polarizer. (C) Uncorrected emission spectra (with parallel polarizer), solid line; corrected, dotted line.

peaks is a necessary indication of an instrument's sensitivity). The position of the Raman peak depends, of course, on the excitation wavelength as shown in Fig. 7B (Fig. 7A shows the Rayleigh scatter, the Raman scatter, and scatter due to the second order of the monochromator). Moreover, because the wavelength scale is not linear with energy, the wavelength difference between the Rayleigh (elastic scatter) and Raman peaks is not fixed. To a useful approximation, the position of the Raman peak (in aqueous solutions) can be calculated by the expression

$$\frac{1}{\lambda_R} = \frac{1}{\lambda_{EX}} - 0.00034 \tag{1}$$

where λ_R and λ_{EX} are the wavelengths of the Raman and excitation peaks, respectively. Figures 7B and 7C make the point that the Raman peaks for aqueous buffers stay fairly constant in intensity and whether they present a concern will depend on

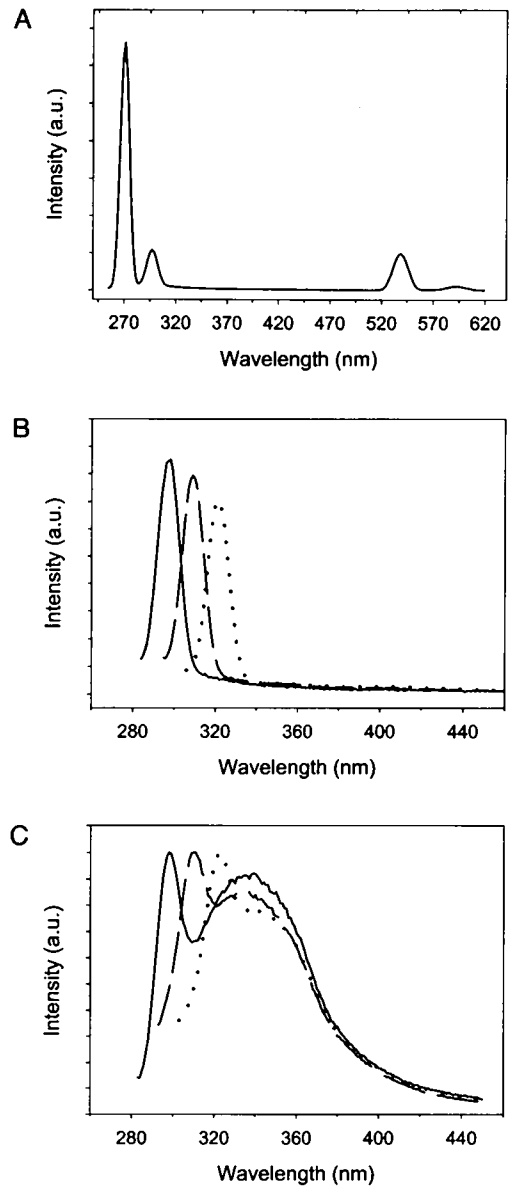

FIG. 7. (A) Emission scan from 250 to 650 nm with excitation at 270 nm; peaks correspond (from left to right) to Rayleigh scatter (270 nm), Raman scatter (297 nm), second-order Rayleigh (540 nm), and second-order Raman (594 nm). (B) Scans of 50 m*M* phosphate buffer, excited at 270 nm (solid line), 280 nm (dashed line), and 290 nm (dotted line). (C) Scans of $\sim 3 \times 10^{-8}$ *M* bovine serum albumin excited at 270 nm (solid line), 280 nm (dashed line), 290 nm (dotted line).

the fluorophore concentration (Fig. 7B also indicates how a "clean" buffer should look relative to the Raman peak for UV excitation). Also shown in Fig. 7C are emission spectra of $\sim 3 \times 10^{-8}\,M$ bovine serum albumin (BSA) excited at three different wavelengths (270, 280, and 290 nm), which show (1) that fluorescence does not change position while the Raman peaks shift and (2) the relative magnitude of the Raman peaks relative to the fluorescence. In the case of tryptophan, one usually can go to about $10^{-7}M$ before worrying about interference from Raman peaks; in the case of fluorophores such as fluorescein, which enjoy robust extinction coefficients and quantum yields, it is possible to work down to about $10^{-9}M$ probe before the Raman peak becomes a concern. (We note that because the Raman peak is highly polarized, care must be taken in some types of polarization studies, involving sample dilution, that increasing polarizations upon decreasing sample signals is not due to the Raman.[14])

It is also worth noting that the most sensitive fluorescence instruments use "photon-counting" methods. Photon counting was originally developed in the 1950s for astronomical photometric observations. It was first applied in fluorescence in the area of lifetime determinations and then in the mid-1970s to steady-state fluorescence measurements.[14,28] The underlying concept of the photon-counting technique is illustrated in Fig. 8 (adapted from Jameson[26]). The advantages of photon counting over direct current measurements include (1) improvement in the signal-to-noise ratio at low light levels, (2) long-term stability, that is, less sensitivity to power supply and amplifier drifts, (3) direct acquisition of data in the digital domain, which facilitates data processing, (4) and effective dynamic range of many orders of magnitude (as determined by the count rate and collection time), and (5) the absolute character of the unit of measurement, that is, photons per unit time. Although photon counting thus offers significant advantages over analog electronics, there is one common pitfall. Namely, it is necessary to be cognizant of the count rate. As shown in Fig. 8, the pulse from the discriminator output has a finite width, which results in an effective instrument dead time. Specifically, if more photons are incident on the system during the time corresponding to a photon pulse they will not be registered, a situation known as "pulse pileup." This fact means that the response of the detector system to incident photons will deviate from linearity as the count rate increases. With modern, fast discriminators the linear count range can extend up to hundreds of thousands of counts per second, but one should be aware of the linear response range for the particular instrument being utilized. Polarization determinations are particularly sensitive to pulse pileup because the parallel intensity component will usually be larger than the perpendicular intensity component and hence will "pile up" first, resulting in an apparent decrease in polarization as the count rate increases.

[28] D. M. Jameson, R. D. Spencer, and G. Weber, *Rev. Sci. Instrum.* **47**, 1034 (1976).

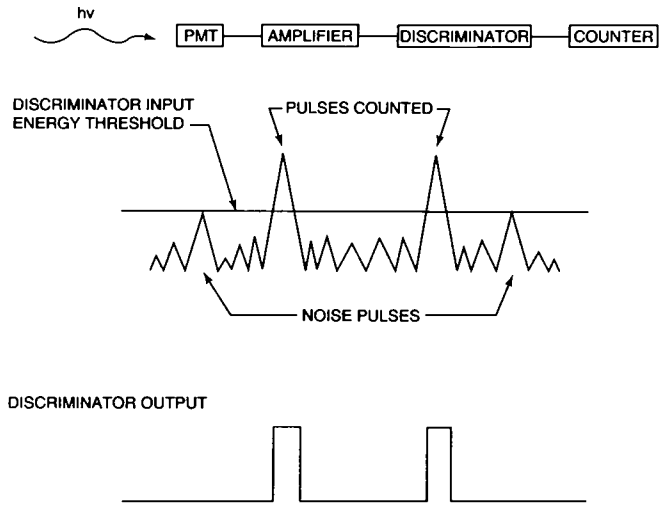

FIG. 8. Schematic illustration of the photon-counting method. Adapted from D. M. Jameson, *in* "Biochemistry." University of Illinois, Champaign-Urbana, IL, 1978.

Excitation Spectra

The relative efficiencies of different wavelengths of incident light to excite fluorophores is determined as the excitation spectrum. In this case, the excitation monochromator is varied while the emission wavelength is kept constant if a monochromator is utilized, or the emitted light can be observed through a filter. If the system is "well-behaved," that is, if the three general rules outlined above hold, the excitation spectrum would be expected to match the absorption spectrum. In this case, however, as in the case of the emission spectrum, corrections for instrumentation factors are required. In fact, excitation spectra not corrected for instrument parameters will deviate seriously from "corrected" excitation spectra, much more so than in the case of emission spectra. This situation is caused by the wavelength-dependent variation in light intensity due to the energy profile of the xenon arc source (Fig. 2). The magnitude of this effect can be seen in Fig. 9A, which depicts the absorption spectrum and the uncorrected excitation spectrum for ANS in ethanol (acquired with an ISS PC1 spectrofluorimeter). Since the xenon arc source produces less light at 280 nm than, for example, 360 nm, the relative heights of these peaks will be distorted from the actual absorption peaks. This effect does not appear in absorption spectra since virtually all absorption spectrophotometers are, in effect, double-beam instruments, which correct for the wavelength dependence of the light source. In the case of the fluorescence excitation spectrum, an approximate correction can be accomplished by using a ratio mode wherein the signal plotted is the sample fluorescence divided by

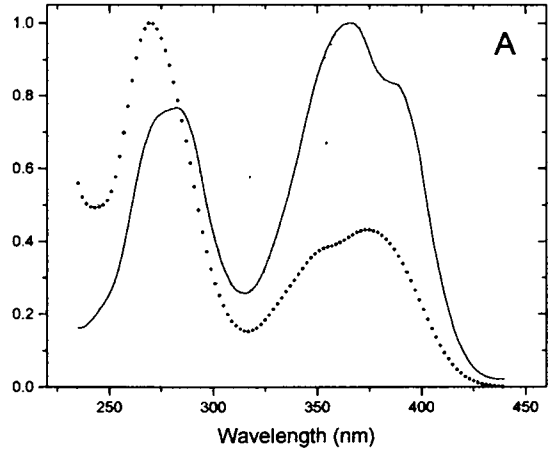
A
1.0
0.8
0.6
0.4
0.2
0.0
250
300
350
400
450
Wavelength (nm)

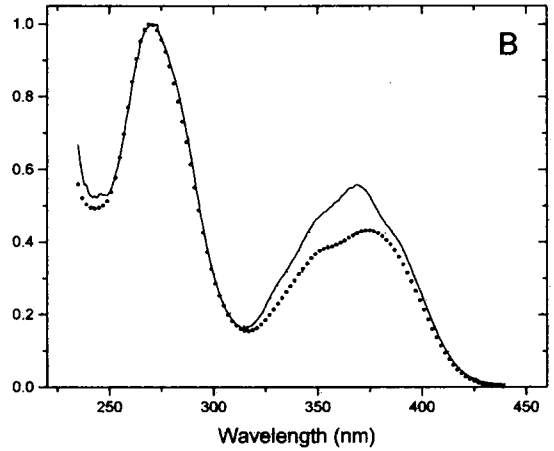
B
1.0
0.8
0.6
0.4
0.2
0.0
250
300
350
400
450
Wavelength (nm)

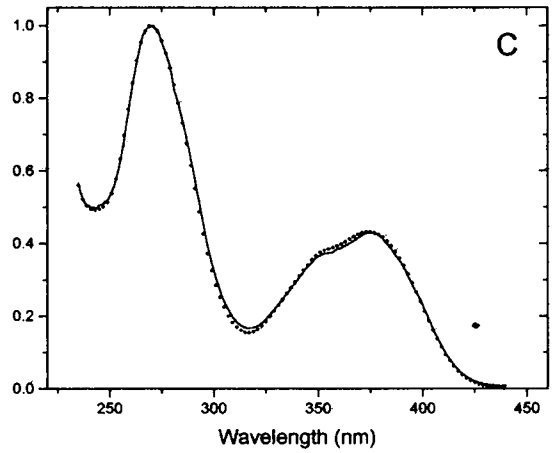
C
1.0
0.8
0.6
0.4
0.2
0.0
250
300
350
400
450
Wavelength (nm)

a reference signal. The reference signal is derived from a small percentage of the excitation beam, which is directed by a quartz beam splitter to a quantum counter (Fig. 1). This quantum counter is typically a concentrated solution of rhodamine B in ethanol placed in a triangular cuvette oriented such that the exciting light strikes the center of the front face of the cuvette while the fluorescence is viewed through a red cut-on filter blocking all light below about 590 nm. In this way, all of the exciting light impinging on the quantum counting solution is absorbed and the fluorescence intensity in the reference channel will reflect the incident light intensity at all excitation wavelengths. The ratio-corrected excitation spectrum for ANS in ethanol is shown in Fig. 9B along with the absorption spectrum. Note that the correspondence between these two spectra is much better than in Fig. 9A but still is not perfect. This small deviation occurs because the quartz beam splitter, used to deflect some light to the reference channel, is not ideal. In fact, the reflectivity of the beam splitter depends on the polarization of the incident light and, as already discussed, the light coming from monochromators will show a wavelength-dependent polarization. Consequently, at wavelengths corresponding to the Wood's anomalies in the excitation monochromator there will be a different ratio of reflected to transmitted light compared with other wavelengths and the "corrected" excitation spectrum will not be properly corrected. To obtain a true corrected excitation spectrum it is necessary to determine the actual lamp profile in the sample compartment, using a quantum counter/front-face arrangement, for example, as was done to obtain the lamp profile shown in Fig. 1. One can then divide the uncorrected sample excitation spectrum by this lamp profile and generate the corrected excitation spectrum as shown in Fig. 9C.

Quantum Yield

The quantum yield (q) of a fluorophore is essentially a measure of how efficiently absorbed light is emitted. The definition of quantum yield and its first direct measurements were due to Vavilov,[29–31] who discovered that fluorescein was an almost perfect emitter with a quantum yield close to unity. One way to view this quantity is that q equals the number of quanta absorbed divided by the number of quanta emitted.

[29] S. I. Vavilov, *Philos. Mag.* **43,** 307 (1922).
[30] S. I. Vavilov, *Z. Physik* **22,** 266 (1924).
[31] S. I. Vavilov, *Z. Physik* **42,** 311 (1927).

FIG. 9. (A) Absorption (dotted line) and uncorrected excitation spectra for ANS in ethanol. (B) Absorption (dotted line) and "ratio"-corrected excitation spectra. (C) Absorption (dotted line) and excitation spectra corrected by a lamp curved as described in text.

A more insightful expression relates the quantum yield to the relative rates of the radiative and nonradiative pathways, which deactivate the excited state. Hence,

$$q = \frac{k_r}{k_r + \sum k_{nr}} \tag{2}$$

where k_r and k_{nr} correspond to radiative and nonradiative processes, respectively. In Eq. (2), $\sum k_{nr}$ designates the sum of the rate constants for the various processes that compete with the emission process. These processes include photochemical and dissociative processes in which the products are well-characterized chemical species (electron, proton, radical, molecular isomer) as well as less well-characterized changes that result in a return to the ground state with simultaneous dissipation of the energy of the excited state into heat. These latter processes are collectively called nonradiative transitions and two types have been clearly recognized: intersystem crossing and internal conversion. Intersystem crossing refers to the radiationless spin inversion of S_1 in the excited state that results in the isoenergetic, or almost isoenergetic, conversion into a triplet state. When spin inversion occurs in S_1 the resulting triplet reached is T_1, which is characterized by an energy intermediate between the ground state and first excited singlet state. Another process that is nonradiative from the point of view of the original excited molecule is resonance energy transfer.

In the past, measurements of quantum yields usually relied on comparison of the intensity of the fluorescence with that of the exciting radiation. The first method of this kind, due to S. I. Vavilov,[30] also had historical interest as it led to the demonstration that fluorescent compounds in solution (fluorescein in the original case) could reradiate most of the absorbed energy rather than a small fraction of it, as many at that time believed. Vavilov, and later Melhuish,[32] used integrating spheres to determine quantum yields. This device is a closed chamber, not necessarily spherical, coated with a light-diffusing material of negligible absorption for the fluorescence and exciting radiation. In practice, a coating of MgO provides good diffusivity and low absorption both in the ultraviolet and visible regions of the spectrum. A detector placed somewhere in the spherical wall samples the radiation density, and it is assumed that conditions are such that homogeneous radiation distribution inside the sphere is reached regardless of the directional emission of the source (diffusing plate or fluorescent sample). A second method of the same type, proposed by Weber and Teale,[33] eliminated the integrating sphere and compared the fluorescent signal with the signal from a nonfluorescent scattering solution, both of which were adjusted to give the same apparent absorbance at the exciting wavelength. These methods of comparison of excitation and fluorescence signals require correction for the difference in spectral response of the photomultiplier

[32] W. H. Melhuish, *J. Phys. Chem.* **65,** 229 (1961).

[33] G. Weber and F. W. J. Teale, *Trans. Faraday Soc.* **53,** 646 (1957).

over the wavelength of excitation and emission, which in turn calls for an exact determination of the molecular fluorescence spectrum. To obviate these sources of error, often underestimated, Weber and Teale interposed between source and photomultiplier a solution of rhodamine B in ethylene glycol intended to act as a proportional quantum counter for the scattering and fluorescent emission.[33] As rhodamine B solutions do not absorb strongly beyond 600 nm this arrangement was limited to fluorophores that did not emit at longer wavelengths.

Interestingly, it is not always necessary to measure emitted light to determine quantum yields because nonradiative processes will lead to dissipation of heat to the solvent, which can be determined calorimetrically. Seybold *et al.*,[34] for example, used an ingenious calorimetric method to measure the thermal expansion of the illuminated fluorescent solution, which was then compared with the larger expansion owing to the nonfluorescent absorber (such as India ink); this volume change could then be directly related to the quantum yield of the fluorophore.

Because the absolute quantum yields of a number of common fluorophores have now been determined, it is usually possible to ascertain the quantum yield of a fluorophore, with adequate accuracy, by comparing its yield relative to a known standard. For example, the quantum yield of tryptophan at 20° at neutral pH is generally taken as 0.14, that of quinine sulfate in 0.1 *N* H_2SO_4 is generally taken as 0.55, and that of fluorescein in 0.01 *N* NaOH is generally taken as 0.94. To ascertain the quantum yield of the fluorophore in question, ideally a solution is made of a standard (such as those listed above) with an optical density matching that of the target fluorophore (note that this step should usually be done via dilutions because accurate optical density measurements are best realized in a range, e.g., near 1, which would cause severe inner filter effects in fluorescence measurements). One then acquires the corrected spectra of standard and target fluorophores, integrate the spectral areas and thus obtain the quantum yield of the target fluorophore is obtained from the ratio of these areas. Tables listing quantum yields with appropriate references for a number of compounds are given on page 160 of Valeur[7] and page 53 of Lakowicz.[24] Vavilov noted[31] that the quantum yield was independent of the excitation wavelength, a conclusion now known as Vavilov's Law. We now appreciate that exceptions to Vavilov's Law can occur. For example, electron ejection from the upper (S_2) level of indole leads to a decrease in the quantum yield at wavelengths below 240 nm.[35,36]

Excited State Lifetimes

In most cases of interest, it is virtually impossible to predict *a priori* the excited state lifetime of a fluorescent molecule. The true molecular lifetime, that is,

[34] P. G. Seybold, M. Gouterman, and J. Callis, *Photochem. Photobiol.* **9,** 229 (1969).
[35] H. B. Steen, *J. Chem. Phys.* **61,** 3997 (1974).
[36] I. Tatischeff and R. Klein, *Photochem. Photobiol.* **22,** 221 (1975).

the lifetime expected in the absence of any excited state deactivation processes, can be approximated by the Strickler–Berg equation.[37]

$$\tau_m^{-1} = 2.88 \times 10^{-9} n^2 \overline{\langle \nu_f^{-3} \rangle} \int_{\Delta \nu_a} \varepsilon(\bar{\nu}) d \ln \bar{\nu} \tag{3}$$

where

$$\overline{\langle \nu_f^{-3} \rangle} = \frac{\int_{\Delta \nu_e} F(\bar{\nu})\, d\nu}{\int_{\Delta \nu_a} F(\bar{\nu}) \nu^{-3}\, d\nu} \tag{4}$$

In these equations, τ_m is the molecular lifetime, n is the refractive index of the solvent, $\Delta \nu_a$ and $\Delta \nu_e$ correspond to the experimental limits of the absorption and emission bands (S_0 to S_1 transitions), respectively, ε is the molar absorption, and $F(\nu)$ describes the spectral distribution of the emission in photons per wavelength interval.

However, the effect of competing radiationless processes that deactivate the excited state (such as quenching, energy transfer, and intersystem crossing) must be taken into account. The relationship between the molecular lifetime (τ_m) and the experimentally observed lifetime (τ_e) is then

$$\tau_e = q \tau_m \tag{5}$$

where q is the quantum yield.

How well do these equations actually work? For NADH in water the equation of Strickler and Berg [Eq. (3)] gives $\tau_m = 76$ ns. Direct measurements yield $\tau = 0.4$ ns and $q = 0.025$, which combined give $\tau_m = 16$ ns. In fact, agreement is rarely better than ~20%.

Fluorescence lifetime measurements are traditionally realized using either the impulse response method (in which excitation is by a brief pulse of light, after which the direct decay of the fluorescence is observed) or the harmonic response method (in which the intensity of the excitation light is modulated sinusoidally and the phase shift of the fluorescence, relative to the excitation, is determined). Direct measurements of fluorescence lifetimes were first successfully realized by the Argentinean E. Gaviola, in Berlin in 1926,[11] following inconclusive efforts by R. W. Wood[38] and P. F. Gottling.[39] Gaviola used a phase fluorometer, which operated at 10 MHz; Gaviola used visual compensation methods to measure the lifetime of aqueous rhodamine (obtaining a value of 2 ns). The mathematical theory behind phase fluorometry did not actually appear until 1933 and was due to Duschinsky.[40] The first use of pulse methods to determine fluorescence lifetimes

[37] S. J. Strickler and R. A. Berg, *J. Chem. Phys.* **37,** 814 (1962).
[38] R. W. Wood, *Proc. R. Soc. A.* **99,** 362 (1921).
[39] P. F. Gottling, *Phys. Rev.* **22,** 566 (1923).
[40] F. Duschinsky, *Z. Physik* **81,** 23 (1933).

is generally credited to Brody.[41] Since these early beginnings, both methods, phase and pulse, have advanced tremendously. Perhaps the most important developments in phase fluorometry were the cross-correlation instrument of Spencer and Weber[42] and the first true variable multifrequency phase and modulation fluorometer built by E. Gratton (originally while a postdoctoral fellow with G. Weber) in the late 1970s.[43] Indeed, the approach taken by Gratton, which revolutionized frequency domain methodologies, was soon adopted by other laboratories and also led to the commercial development of the method by ISS (Champaign, IL). Important developments in the pulse method included the use of time-correlated single photon counting and the appearance of ultrafast pulsed laser sources, which rendered moot much of the effort that had been expended on deconvolution techniques. Despite these impressive advances in the pulse method, however, it must be said that W. R. Ware erred when he predicted at the 1980 NATO *Advanced Studies Meeting on Time-Resolved Fluorescence in Biochemistry and Biology*[44] that "the use of mode-locked, synchronously pumped dye laser excitation sources, with or without frequency doubling, in conjunction with single-photon detection, would seem to be the final nail in the phase-shift coffin. . . ." In fact, multifrequency phase and modulation fluorometry is widely utilized both for normal solution studies as well as for fluorescence lifetime microscopy. These frequency domain methods have also found increasing applications in diagnostic imaging (see, e.g., Stankovic *et al.*[45] or the web site www.iss.com).

Interestingly, one form of phase and modulation fluorometry utilizes pulsed sources for excitation. The possibility of using the harmonic content of high-repetition rate-pulsed light sources for phase/modulation fluorometry was discussed by Gratton and Lopez-Delgado[46] and one of the first implementations of the method used the Frascati synchrotron radiation source ADONE.[47] The concept underlying this approach is that repetitive pulse sources have a harmonic content, as dictated by Fourier and Laplace transforms, which can be used to generate multiple frequencies for phase and modulation measurements. The main difference between the use of external modulating devices, such as Pockels cells, and the harmonic content of a repetitive light source, such as synchrotron radiation or a mode-locked laser, is that in the latter case the researcher is limited to frequencies that are multiples of the fundamental repetition rate (of course, these frequencies

[41] S. S. Brody, *Rev. Sci. Instrum.* **28,** 1021 (1957).
[42] R. D. Spencer and G. Weber, *Ann. N.Y. Acad. Sci.* **158,** 361 (1969).
[43] E. Gratton and M. Limkeman, *Biophys. J.* **44,** 315 (1983).
[44] W. R. Ware, *in* "Time-Resolved Spectroscopy in Biochemistry and Biology" (R. B. Cundall and R. E. Dale, eds.), Vol. 69, p. 23. Plenum Press, New York, 1983.
[45] M. R. Stankovic, D. Maulik, W. Rosenfeld, P. G. Stubblefield, A. D. Kofinas, E. Gratton, M. A. Franceschini, S. Fantini, and D. Hueber, *J. Matern. Fetal Med.* **9,** 142 (2000).
[46] E. Gratton and R. Lopez-Delgado, *Il Nuovo Cimento* **56B,** 110 (1980).
[47] E. Gratton, D. M. Jameson, N. Rosato, and G. Weber, *Rev. Sci. Instrum.* **55,** 486 (1984).

can also be modulated externally by using electro-optical devices). For example, the fundamental frequency of the original source at the Frascati Electron Storage Ring, ADONE (operating in the single bunch mode), was 2.886167 MHz, which then gave rise to a set of harmonic frequencies (a comb function) set 2.886167 MHz apart. The intensities characteristic of this frequency set fit a Gaussian envelope with a half-width of 500 MHz (the inverse of 2 ns, the FWHM of the Gaussian pulse width). After the original proof of concept at Frascati, the harmonic content approach to phase and modulation measurements was used in conjunction with a mode-locked laser-based instrument.[48]

The basic principles of both frequency domain and time domain approaches to fluorescence lifetime determinations have been reviewed many times and we refer readers with a sustaining interest to these accounts (e.g., see Refs. 7, 24, and 49–51). We shall, instead, remind the reader of a fundamental aspect of lifetime determinations that is relevant to either method. Specifically, we refer to the use of the so-called magic angles. This effect was discussed by Spencer and Weber,[52] who drew attention to the fact that observation of the fluorescence at 90° to the excitation will weigh the vertically polarized component relative to horizontally polarized components (because when viewed in this manner one of the horizontal components cannot be observed), so that the measured lifetime will deviate slightly from the true molecular lifetime. This effect is usually small but can, in extreme cases, be as much as 10–15%.[52] This artifact, however, can be avoided through the use of specific conditions for excitation and emission. Namely, four "magic angle" conditions that eliminate polarization bias are as follows: (1) 35° excitation, no emission polarizer; (2) natural excitation, 35° emission polarizer; (3) 55° excitation polarizer, parallel (0°) emission polarizer; and (4) parallel (0°) excitation polarizer, 55° emission polarizer. In practice, at least with the frequency domain approach, researchers typically use method 4 because the modulated excitation is usually generated with a Pockels cell and a polarizer, which will produce a parallel polarization. The advantage of this method is also that the sample and reference signals (used to generate the phase shift and demodulation ratio) both will be viewed through a polarizer oriented at 55°, which can eliminate any polarization bias in the PMT.

As time-resolved instrumentation improved over the years, so did the mathematical approaches to analysis. In the 1970s, a tremendous effort was expended on development of methods to deconvolute and fit pulse decay data; many of these

[48] R. J. Alcala, E. Gratton, and D. M. Jameson, *Anal. Instrum.* **14,** 225 (1985).
[49] J. N. Demas, "Excited State Lifetime Measurements." Academic Press, New York, 1983.
[50] D. M. Jameson, E. Gratton, and R. D. Hall, *Appl. Spectrosc. Rev.* **20,** 55 (1984).
[51] D. M. Jameson and T. L. Hazlett, *in* "Biophysical and Biochemical Aspects of Fluorescence" (G. Dewey, ed.), p. 105. Plenum Press, New York, 1991.
[52] R. D. Spencer and G. Weber, *J. Chem. Phys.* **52,** 1654 (1970).

methods are discussed in the book that resulted from the 1978 NATO conference,[53] which was one of the first large international meetings devoted exclusively to time-resolved fluorescence. As flash lamps began to give way to shorter and shorter laser pulses, however, many of these deconvolution methods became moot because the majority of the systems being studied had lifetimes that were long, compared with the duration of the exciting pulse. The present availability of femtosecond pulses means that special deconvolution techniques are required only in rare cases.

Analysis of lifetime data has, in fact, been developing in other directions than originally envisaged at that NATO conference. For example, software has been developed (largely from the Gratton laboratory[54–56]) that allows the fitting of lifetime data to distribution models, as opposed only to sums of discrete exponentials. The original motivation for this development was to try to rationalize the lifetime heterogeneity observed in single-tryptophan proteins in terms of dynamic aspects of the protein matrix. Also, both frequency domain and time domain approaches have taken advantage of global analysis approaches.[57,58] These approaches allow the linking of various lifetime properties among sets of data, which often reveals trends and associations that were not originally apparent and that often significantly improve the precision of the resolved components. Another relatively recent approach is the maximum entropy method (MEM), which uses "model-less" fits of the lifetime data (usually time domain data) to reveal the underlying decay kinetics.[59–61] The choice of whether to use either the MEM approach or direct model-fitting approaches[50,54–56,58] is actually more of a philosophical choice because some people prefer to evaluate their data against a particular model whereas others prefer to avoid the constraints of models altogether.

Finally, we should note that time-resolved methods, using essentially the same instrumentation used to acquire intensity decay data, have also been developed to acquire direct hydrodynamic information about fluorescent systems. In other words, rotation properties of fluorophores and the system they monitor can be obtained by so-called time-decay anisotropy or dynamic polarization measurements. These methods have been reviewed extensively[7,24,51,62] and we shall not discuss them further.

[53] R. B. Cundall and R. E. Dale, eds., "NATO ASI Series, Series A: Life Sciences," Vol. 69. Plenum Press, New York, 1983.
[54] J. R. Alcala, E. Gratton, and F. G. Prendergast, *Biophys. J.* **51,** 925 (1987).
[55] J. R. Alcala, E. Gratton, and F. G. Prendergast, *Biophys. J.* **51,** 597 (1987).
[56] J. R. Alcala, E. Gratton, and F. G. Prendergast, *Biophys. J.* **51,** 587 (1987).
[57] J. M. Beechem, J. R. Knutson, and L. Brand, *Biochem. Soc. Trans.* **14,** 832 (1986).
[58] J. M. Beechem, M. Gratton, J. R. Knutson, and W. W. Mantulin, *in* "Topics in Fluorescence Spectroscopy II" (J. R. Lakowicz, ed.), p. 241. Plenum Press, New York, 1991.
[59] A. K. Livesey and J.-C. Brochon, *Biophys. J.* **52,** 693 (1987).
[60] J.-C. Brochon, A. K. Livesey, J. Pouget, and B. Valeur, *Chem. Phys. Lett.* **174,** 517 (1990).
[61] J.-C. Brochon, *Chem. Phys. Lett.* **174,** 517 (1990).
[62] E. Gratton, D. M. Jameson, and R. D. Hall, *Annu. Rev. Biophys. Bioeng.* **13,** 105 (1984).

Polarization/Anisotropy

The linear polarization (p) of a beam of light may be defined as the ratio of the intensity of the polarized light (P) to the total light, that is, natural (N) plus polarized, N being characterized by $P = 0$.

$$p = \frac{P}{P + N} \tag{6}$$

This definition presupposes the absence of elliptically polarized light in the light beam, which can then be considered for our purpose as a mixture of natural and linearly polarized light. This case is entirely correct for the radiation emitted by optically inactive molecules and all but correct for emission by an optically active molecule, as in this case the fraction of circularly polarized light in the emission does not generally exceed one-thousandth of the total.

If $I_{\parallel}$ is defined as the intensity seen through a polarizer set to maximally transmit P, and $I_{\perp}$ is at 90° to this direction, thus excluding P, then

$$I_{\parallel} - I_{\perp} = P \tag{7}$$

$$I_{\parallel} + I_{\perp} = P + N \tag{8}$$

and hence

$$p = \frac{I_{\parallel} - I_{\perp}}{I_{\parallel} + I_{\perp}} \tag{9}$$

Thus, the linear polarization, or fraction of linearly polarized light in a beam, is measured by setting a polarizer in two positions at 90° from each other, one of these two positions being set so as to obtain maximum intensity. The sign of the polarization is a matter of convention. It is possible to speak of positive and negative polarizations of the fluorescence because $I_{\parallel}$ is chosen to coincide with the electric vector of the exciting light and the definition of p of Eq. (9) is used in every case. The polarization of the fluorescence from a source is regarded as positive if the greater fluorescence intensity is polarized parallel to the polarization of the excitation, that is, $I_{\parallel} > I_{\perp}$ and negative if the greater fluorescence intensity is polarized normal to the polarization of the excitation that is, $I_{\parallel} < I_{\perp}$. As a matter of practical significance, to properly determine polarization values the researcher must correct for any bias in the detector arm (either due to monochomator or PMT response) and this operation is accomplished by measuring the parallel and perpendicular polarized intensities of the emission while exciting with perpendicularly polarized light, that is, in a direction that is orthogonal to both emission components (due to the right-angle observation). This symmetrical excitation arrangement means that the two emission polarization components should be equal, and hence any deviation from equality can be ascribed to a bias and corrected. Although this principle was recognized early on in polarization research it is now usually referred to as the

"G factor" after the nomenclature of Azumi and McGlynn,[63] who used this term to refer to the bias of the grating in the emission monochromator.

The polarization of dilute solutions of fluorescein in water was first reported by F. Weigert in 1920,[64] who pointed out that the polarization value depended on the molecular size of the fluorophore and the viscosity of the medium. The correct quantitative relation between the observed polarization and parameters such as the excited state lifetime, the size of the fluorophore, and the viscosity of the solution was enunciated by F. Perrin in 1926[65] (for an excellent discussion of the outstanding contributions of J. and F. Perrin to fluorescence the reader is directed to the article by Berberan-Santos[5]). In this classic 1926 article, the equation, now known as the Perrin equation, first appears as

$$p = p_0 \frac{1}{1 + \left(1 - \frac{1}{3}p_0\right)\frac{RT}{V\eta}\tau} \tag{10}$$

where p is the polarization, p_0 is the limiting polarization (in the absence of rotation), R is the universal gas constant, T is the absolute temperature, V is the molar volume of the rotating unit, η is the solvent viscosity, and τ is the excited state lifetime. Equation (10) is now usually written as

$$\frac{1}{p} - \frac{1}{3} = \left(\frac{1}{p_0} - \frac{1}{3}\right)\left(1 + \frac{RT}{V\eta}\tau\right) \tag{11}$$

This expression is often further simplified to

$$\frac{1}{p} - \frac{1}{3} = \left(\frac{1}{p_0} - \frac{1}{3}\right)\left(1 + \frac{3\tau}{\rho}\right) \tag{12}$$

where ρ is the Debye rotational relaxation time, which for a sphere is given as

$$\rho_0 = \frac{3\eta V}{RT} \tag{13}$$

In the case of a protein wherein the partial specific volume (ν) and hydration (h) are known, Eq. (14) can then be written

$$\rho_0 = \frac{3\eta M(\nu + h)}{RT} \tag{14}$$

where M is the molecular weight, ν is the partial specific volume, and h is the degree of hydration. For a spherical protein of molecular mass 44 kDa, with a

[63] T. Azumi and S. P. McGlynn, *J. Phys. Chem.* **37,** 2413 (1962).
[64] F. Weigert, *Verh. Dtsch. Chem. Ger.* **23,** 100 (1920).
[65] F. Perrin, *J. Phys.* **7,** 390 (1926).

partial specific volume of 0.74 and hydration of 0.3 ml/mg at room temperature, $\rho = (3)(0.01)(44000)(0.74 + 0.3)/(8.31 \times 10^7)(293) = \sim 56$ ns. So to a rough approximation, the Debye rotational relaxation time (in nanoseconds) for a spherical protein is close to its molecular mass. Of course, for nonspherical particles, which may be approximated as hydrodynamically equivalent prolate or oblate ellipsoids, the equation is more complicated and considers the harmonic mean of the rotational relaxation times about the three principle axes of rotation.[9,66] We should comment here on the term "rotational correlation time," often denoted as τ_c. In fact, $\rho = 3\tau_c$, a fact that stems from the original definitions of these terms. As pointed out previously,[67] the rotational relaxation time was originally defined by Debye in relation to dielectric dispersion, in which the relevant orientational distribution is a function of $\cos\theta$, where θ is the angle between the direction of the electric field and the molecular dipole axis. Perrin used this approach of Debye when deriving the characteristic time for molecular rotation of spheres. Much later, Bloch derived equations for computing the decay of nuclear polarizations and used a slightly different approach, which yielded a characteristic time that was one-third the Debye rotational relaxation time, that is, the correlation time. It is, in fact, possible to use the function known as anisotropy (r), which is defined as

$$r = \frac{I_{\parallel} - I_{\perp}}{I_{\parallel} + 2I_{\perp}} \tag{15}$$

and recast the Perrin equation as

$$\frac{r}{r_0} = 1 + \frac{\tau}{\tau_c} \tag{16}$$

where r_0 is the limiting anisotropy and τ_c is the rotational correlation time as discussed above. The simplified form of this equation, compared with the original Perrin equation, has attracted users. We simply want to stress that the information content of the various terms, polarization/anisotropy or relaxation time/correlation time, is identical and the most important consideration is to clearly specify which terms are being used. We also leave to the reader to prove, given the definition of anisotropy, that the following two equations hold:

$$r = \frac{2}{3}\left(\frac{1}{P} - \frac{1}{3}\right)^{-1} \tag{17}$$

$$r = \frac{2P}{3 - P} \tag{18}$$

[66] D. M. Jameson and S. E. Seifried, *Methods* **19,** 222 (1999).

[67] D. M. Jameson and W. H. Sawyer, *Methods Enzymol.* **246,** 283 (1995).

Francis Perrin had actually also introduced the quantity $2p/(3 - p)$,[5,68] and this function was later named "anisotropy" by Jabłoński.[69] Curiously, Jabłoński never acknowledged the use by Perrin of this function. Similarly, when Jabłoński published in 1960 on the additivity of anisotropy,[70] he neglected to cite the 1952 article by G. Weber,[9] which explicitly gave the formulation for the additivity of polarization, and from which the Jabłoński equation followed in a trivial fashion.

Polarization measurements are usually used to acquire information about the rotational motions of probes, either to gain knowledge about the viscosity of the medium or to understand hydrodynamic aspects of the system. This latter consideration has been widely applied to study macromolecular associations (such as protein–protein or protein–nucleic acid) as well as ligand binding.[66,67] In fact, one of the most widely used techniques in clinical assays for drugs or metabolites is the fluorescence polarization immunoassay, using the Abbott (Abbott Park, IL) TDx instrument (www.abbottdiagnostics.com). Interestingly, in this approach Abbott adopted the nomenclature of the "millipolarization" unit, a term that is also now widely used in fluorescence plate readers and that is, simply, the polarization times 1000. When the TDx system first came out in the early 1980s one of us (D.M.J.) asked some of the principal developers of the system why the term millipolarization was used, as, of course, polarization is a unitless number. The response was that many of the potential end-users of the TDx system were concerned about the traditional nomenclature because changes in polarization of, say, 0.20 to 0.30 did not seem very large. But when these numbers were given as millipolarization units, that is, 200 to 300 mps, then these same end-users were impressed!

As discussed below, polarization data can also be used to study energy transfer processes. One other use of polarization data seems worthy of comment, however, because it lies at the heart of the method. Namely, the so-called limiting polarization (P_0 in the Perrin equation), that is, the polarization in the absence of rotation or energy transfer, gives a measure of the angle between the absorption and emission dipoles. As derived elsewhere,[7,71] the limits for polarization from a solution of randomly oriented fluorophores are $+1/2$ and $-1/3$, depending on whether the absorption and emission dipoles are collinear ($+1/2$) or orthogonal ($-1/3$). The expression relating the limiting polarization to this angle is

$$\frac{1}{P_0} - \frac{1}{3} = \frac{5}{3}\left(\frac{2}{3\cos^2\phi - 1}\right) \tag{19}$$

This method is, in fact, one of the few that can be used to gain knowledge of the relative orientation of these dipoles (see, e.g., Valeur[7] for some examples). The

[68] F. Perrin, *Acta Phys. Polon.* **5**, 335 (1936).
[69] A. Jabłoński, *Acta Phys. Polon.* **17**, 471 (1957).
[70] A. Jabłoński, *Bull. Acad. Polon. Sci. Serie Sci. Math. Astron. Phys.* **6**, 259 (1960).
[71] G. Weber, *in* "Fluorescence and Phosphorescence" (D. Hercules, ed.), p. 217. John Wiley & Sons, New York, 1966.

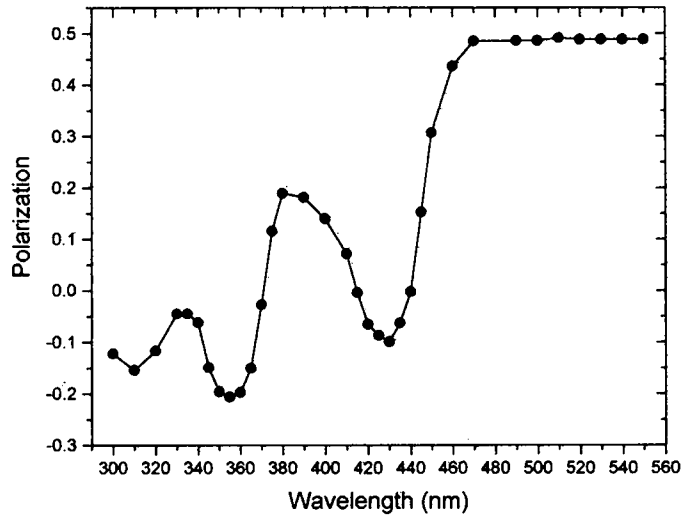

FIG. 10. Excitation polarization spectra of rhodamine B embedded in a Lucite matrix at room temperature. Emission was viewed through a cut-on filter passing wavelengths longer than 560 nm; slits were ~4 nm. The instrumentation utilized is described in D. M. Jameson, G. Weber, R. D. Spencer, and G. Mitchell, *Rev. Sci. Instrum.* **49,** 510 (1978).

basic idea is that as the excitation wavelength is varied and different electronic states are reached (Fig. 3), the direction of the corresponding absorption transition dipoles varies and, because emission is always from the same dipole regardless of which level is initially excited, the observed polarization will vary depending on the original angle between the absorption and emission dipoles. This fact means, of course, that care must be exercised concerning which excitation wavelength is used for polarization studies—a point often overlooked because most practitioners simply excite into the final absorption band, which will usually have the highest P_0. As shown in Fig. 10, for the case of immobilized rhodamine B, the variation of polarization with wavelength (known as the excitation polarization spectrum) can be profound. Yet, if the limiting polarization at the wavelength utilized is known, the same type of measurements can be carried out even if the limiting polarization is negative (see, e.g., VanderMeulen *et al.*[72]). Finally, we should mention that the polarization across the emission spectrum is almost always constant (which is why cut-on filters can be used to collect the entire emission and hence gain in sensitivity), but a few cases occur (e.g., pyrene) wherein the polarization will vary with emission wavelength and hence the choice of observation wavelength or filter is critical.

[72] D. L. VanderMeulen, D. G. Nealon, E. Gratton, and D. M. Jameson, *Biophys. Chem.* **36,** 177 (1990).

Fluorescence Resonance Energy Transfer, Specifically Fluorescence Resonance Energy Transfer between Identical Molecules

As mentioned earlier, a wealth of articles dealing with heterotransfer have appeared, and readers interested in this area may consult various sources.[7,24,73–77] Energy transfer was noted as early as 1922 by Cario and Franck,[78] who observed that irradiation of mixtures of mercury and thallium vapors, with a wavelength absorbed by mercury but not by thallium, resulted in emission from both atoms. Hence, a nonradiative transfer mechanism was required. One topic in energy transfer that has not been extensively discussed, however, is homo-FRET (fluorescence resonance energy transfer between identical molecules). In the case of homo-FRET, as opposed to hetero-FRET, the transfer efficiency cannot be quantified by observation of the decrease in the donor intensity (or lifetime) and/or increase in the acceptor intensity, because donor and acceptor are the same. Nonetheless, transfer efficiency, and hence distance, information can be obtained by monitoring the polarization of the emission. One of the few reviews in this area was provided in 1983 by Kawski,[79] who dealt mainly with homotransfer between fluorophores in isotropic media. Valeur also considers homo-FRET.[7] We should also mention that the use of the word "fluorescence" in the phrase "fluorescence resonance energy transfer" is somewhat of a misnomer because the "fluorescence" itself is not transferring.

The first report on homo-FRET was by Gaviola and Pringsheim,[80] who noted that an increase in the concentration of dyes in viscous solvent was accompanied by a progressive depolarization, even at concentrations where self-quenching was still negligible. Francis Perrin recognized this phenomenon as a special case of fluorescence energy transfer: *"L'existence de transferts d'activation est expérimentalement prouvée pour de telles molécules par la décroissance de la polarisation de la lumière de fluorescence quand la concentration croit (aucune dépolarisation ne peut résulter dans une solution très visqueuse d'une rotation des molécules, qui exigerait, pour se produire en un temps de l'ordre de la durée moyenne d'émission, une énergie plus grande que l'énergie d'activation toute entière)"*. ["The existence

[73] H. C. Cheung, *in* "Topics in Fluorescence Spectroscopy" (J. R. Lakowicz, ed.), Vol. 3, p. 127. Plenum Press, New York, 1991.

[74] R. M. Clegg, *in* "Fluorescence Imaging Spectroscopy and Microscopy" (X. F. Wang and B. Herman, eds.), Vol. 137, p. 179. John Wiley & Sons, New York, 1996.

[75] C. G. dos Remedios and P. D. J. Moens, *in* "Resonance Energy Transfer" (D. L. Andrews and A. A. Demidov, eds.), p. 1. John Wiley & Sons, New York, 1999.

[76] B. W. Van Der Meer, G. Coker, and S.-Y. S. Chen, "Resonance Energy Transfer: Theory and Data." Wiley-VCH, New York, 1991.

[77] P. Wu and L. Brand, *Anal. Biochem.* **218,** 1 (1994).

[78] G. Cario and J. Franck, *Z. Physik* **11,** 161 (1922).

[79] A. Kawski, *Photochem. Photobiol.* **38,** 487 (1983).

[80] E. Gaviola and P. Pringsheim, *Z. Physik* **24,** 24 (1924).

of transfer of activation is proven experimentally for such molecules by the decrease in polarization of the fluorescent light when the concentration is increased (in a very viscous solution, no depolarization can result from the rotation of the molecules, which would require, to occur in a time of the order of the mean lifetime of the emission, a greater energy than the whole activation energy).”][81] In this article, F. Perrin gave a quantum mechanical theory of energy transfer between like molecules in solution. He also presented a qualitative discussion of the effect of the spectral overlap between the emission spectrum of the donor and the absorption spectrum of the acceptor (in the case of like molecules), which could explain the difference between the calculated distance at which the transfer of activation occurs and the distance inferred from the polarization observations. *“Il est vraisemblable que cet écart est dû à l'étalement des fréquences d'absorption et d'émission, sur des bandes spectrales assez larges n'empiétant qu'assez peu l'une sur l'autre. Cet étalement, dû aux possibilités de vibrations mécaniques internes des molécules, et au couplage très fort de ces vibrations avec l'agitation thermique du solvant, diminue considérablement la grandeur des moments associés aux transitions à la fois pour les deux molécules en présence.”* [“It is reasonable to think that this gap is due to the spreading of the absorption and emission frequency, over spectral bands sufficiently large and overlapping only slightly. This spreading, resulting from possible internal mechanical vibrations, and from the very strong coupling of these vibrations to the thermal agitation of the solvent, considerably reduces the size of the moment associated with the possible simultaneous transitions for the two molecules considered.”][81] Several years later, Förster[82,83] published the first quantitative theory of molecular resonance energy transfer.

Depolarization Due to Energy Transfer

At the Tenth Spiers Memorial Lecture of the Faraday Society, Förster reported that “excitation transfer between alike molecules can occur in repeated steps. So the excitation may *migrate* from the absorbing molecule over a considerable number of other ones before deactivation occurs by fluorescence or some other process. Though this kind of transfer cannot be recognized from fluorescence spectra, it may be observed by the decrease of fluorescence polarization. . . .”[84]

Depolarization of fluorescence can occur either because of Brownian rotations (discussed earlier) or because of energy transfer (Fig. 11); the excited fluorophore transfers energy, in a radiationless process, to an acceptor (with absorption and emission dipole moments oriented differently from the donor molecule), which

[81] F. Perrin, *Ann. Phys.* **XVII,** 283 (1932).
[82] T. Förster, *Naturwissenschaften* **6,** 166 (1946).
[83] T. Förster, *Ann. Phys. (Leipzig)* **2,** 55 (1948).
[84] T. Förster, “Discussions of the Faraday Society,” Vol. 27, p. 7. Aberdeen University Press, Aberdeen, Scotland, 1960.

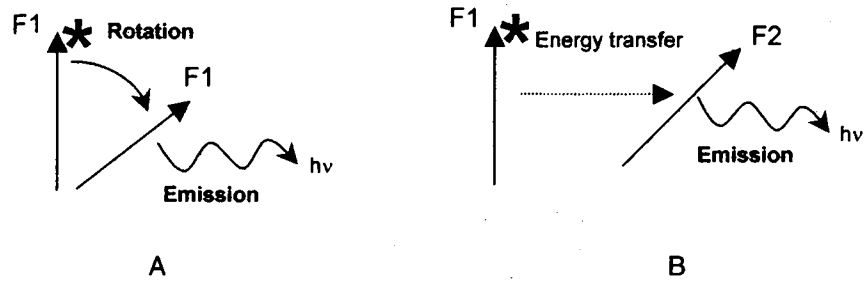

FIG. 11. (A) Depolarization resulting from rotational diffusion of a fluorophore. (B) Depolarization resulting from homo-FRET.

in turn emits a photon. Of course, these two processes can occur simultaneously and hence may both contribute to depolarization of the emitted light. Unlike heterotransfer, and apart from the fact that multiple energy transfer events can occur before an acceptor molecule finally emits the photon, back transfer can also occur from the excited acceptor molecule to the originally excited donor, a process that limits the depolarization of the emitted light. If the rate of transfer from the donor molecule to the acceptor is equal to the rate of back transfer from the acceptor molecule to the donor molecule, the minimum value of anisotropy reached, in the case of 100% transfer efficiency, is roughly equal to the anisotropy in the absence of energy transfer divided by the number of chromophores (see below). However, the rate of back transfer is not necessarily equal to the rate of forward transfer. For instance, energy transfer from fluorophores with higher quantum yields, and therefore longer lifetimes, to those with smaller quantum yields and shorter lifetimes will occur more often than the converse process.

Homo-FRET does not, to a first approximation, result in changes in the overall fluorescence intensities and lifetimes of the fluorophores. Also, unlike depolarization due to Brownian motions, depolarization from homo-FRET is temperature independent. For some fluorophores (see below), there is a failure of energy transfer when the fluorophores are excited on the red edge of their excitation band[85,86] (also reviewed in Valeur[7]).

Homo-FRET for Fluorophores in Isotropic Media

When homo-FRET occurs in viscous solution, it can be detected by the concentration depolarization of fluorescence.[80] In 1954, Weber showed that the reciprocal of the polarization is a linear function of the concentration of the fluorescent

[85] G. Weber, *Biochem. J.* **75,** 335 (1960).
[86] G. Weber and M. Shinitzky, *Proc. Natl. Acad. Sci. U.S.A.* **65,** 823 (1970).

molecules.[87] Weber also showed[71,87] that it was possible to calculate the distance R_0 (i.e., the critical Förster distance; the distance at which the probability of emission equals the probability of transfer) by the following equations:

$$\frac{1}{P} - \frac{1}{3} \approx \left(\frac{1}{P_\infty} - \frac{1}{3}\right)\left[1 + 1.68\left(\frac{R_0}{2a}\right)^6 C\right] \tag{20}$$

where P is the polarization at concentration C, P_∞ is the polarization at infinite dilution, and $2a$ is the distance of closest approach of any molecule to the excited molecule (a is the molecular radius). R_0 can be obtained from the slope of the straight line obtained (in a thin layer in which radiative transfer is negligible) when $(1/P) - (1/3)$ is plotted against the concentration C. Depolarization in thick layers gives rise to an upward curvature of the line (instead of a straight line) when $(1/P) - (1/3)$ is plotted against the concentration because of the radiative transfer in more concentrated solution, which increases the degree of depolarization. This approach was used to calculate the R_0 values for various fluorophores in solution.[71,85,87]

Another approach was described by Kawski and Nowaczyk.[88] They generalized the simple active sphere model proposed by Jabłoński[89] to take into account the mutual orientation of the donor and acceptor transition dipole moment. In this treatment, a luminescent center is assumed to consist of donor surrounded by a shell of volume V within which a number of identical unexcited molecules (acceptors) can be found [$V = (4/3)\pi(R_s^3 - a^3)$, where a is the minimum separation at which the contribution of the Förster interaction to the excitation energy transfer is maximum and R_s is the effective range of the Förster interaction[79]]. Assuming that the rate of transfer is equal to τ^{-1}, the normalized anisotropy is given by

$$\frac{r}{r_0} = \frac{2(\nu - 1 + e^{-\nu})}{\nu^2} \tag{21}$$

where the mean number of acceptors (ν) within the shell is expressed by

$$\nu = \frac{4}{3}\pi R_s^3\left[1 - \langle\kappa^2\rangle\left(\frac{R_0}{R_s}\right)^6\right]n \tag{22}$$

where n is the fluorophore concentration per milliliter and κ^2 is the well-known orientation factor (see, e.g., Van Der Meer *et al.*[76]).

Kawski[79] calculated R_0 for several fluorophores, using this modified simple sphere model, and showed that there was good agreement between the calculated values and those obtained from the absorption and emission spectral overlap of these dyes.

[87] G. Weber, *Trans. Faraday Soc.* **50,** 552 (1954).
[88] A. Kawski and K. Nowaczyk, *Acta Phys. Polon.* **A54,** 777 (1978).
[89] A. Jabłoński, *Acta Phys. Polon.* **14,** 295 (1955).

For two-dimensional systems, the mean number of acceptor molecules is given by Eq. (23)[88]:

$$v = \pi R_s^2 \left\{ 1 - \frac{R_0^3 \langle \kappa^2 \rangle}{6R_s^6} \left[\frac{R_0^3}{2} + \left(\frac{R_0^6}{4} + \frac{2R_s^6}{\langle \kappa^2 \rangle} \right)^{1/2} \right] \right\} n \tag{23}$$

Homotransfer in Proteins and Peptides

Weber[90] was the first to study the polarization spectra of proteins containing tyrosine and/or tryptophan. He showed that homo-FRET between tyrosine residues was responsible for the low polarization values of the proteins compared with the polarization values of tyrosine solutions. Similarly, in proteins containing tryptophan, Weber noted that the polarization values at 270 nm were lower than that of *N*-glycyltryptophan. Homotransfer was also found to be the sole factor contributing to the decrease in polarization with the increase in the number of 1-anilino-8-naphthalene sulfonate molecules adsorbed on the same bovine serum albumin molecule.[91–93]

The homotransfer method was applied to protein oligomers to study dissociation and subunit exchange under pressure.[94–96] Both heterotransfer and homotransfer permit qualitative detection of the dissociation and subunit exchange of the oligomers, but only homotransfer allows a direct quantitative estimate of both processes.[94] When labeled proteins are in the presence of a large excess of unlabeled proteins and the pressure is raised from atmospheric to that required for half-dissociation, the polarization increases because of two different processes: (1) dissociation (which places the dissociated fraction at distances at which transfer is negligible) and (2) exchange of labeled subunits with unlabeled subunits. Assuming the independence of these two causes of change in polarization,[94]

$$r_x(t) = r_1 + (r_s - r_1)\left(1 - \exp^{-t/\tau_x}\right) \tag{24}$$

$$r_\alpha(t) = r_1 + (r_s - r_1)\left(1 - \exp^{-t/t_1}\right) \tag{25}$$

where $r_\alpha(t)$ is the anisotropy change due to dissociation with a time constant t_1, $r_x(t)$ is the anisotropy change following the replacement of fully labeled oligomers by others carrying a single labeled subunit with a characteristic time (τ_x) for reduction of the unscrambled subunit fraction to e^{-1} of its original value, r_1 is the observed decreased emission anisotropy, and r_s characterizes the emission

[90] G. Weber, *Biochem. J.* **75,** 345 (1960).
[91] G. Weber and L. Young, *J. Biol. Chem.* **239,** 1415 (1964).
[92] G. Weber and E. Daniel, *Biochemistry* **5,** 1900 (1966).
[93] G. Weber and S. R. Anderson, *Biochemistry* **8,** 361 (1969).
[94] L. Erijman and G. Weber, *Biochemistry* **30,** 1595 (1991).
[95] L. Erijman and G. Weber, *Photochem. Photobiol.* **57,** 411 (1993).
[96] K. Ruan and G. Weber, *Biochemistry* **32,** 6295 (1993).

anisotropy of both dissociation and complete exchange. The observed emission anisotropy $r(t)$ is a weighted average of $r_\alpha(t)$ and $r_x(t)$:

$$r(t) = \alpha r_\alpha(t) + (1 - \alpha) r_x(t) \tag{26}$$

Self-Association of Peptides within Lipid Bilayer

MacPhee *et al.*[97] showed evidence of peptide self-association, resulting from an increase in the peptide-to-surface density, using homotransfer between amphipathic α-helices derived from apolipoprotein C-II labeled with 7-nitrobenz-2-oxa-1,3-diazole (NBD). They followed the work of Wobler and Hudson,[98] which predicted the energy transfer efficiencies for heterotransfer between donors and acceptors randomly distributed on a two-dimensional surface as a function of fluorophore surface density. Several assumptions were made to accommodate for homotransfer.

1. *The fluorescence anisotropy is primarily determined by the initially excited donor molecule and a single transfer event is sufficient to cause complete depolarization of the light emitted from the acceptor.* This assumption followed from the work of Agranovich and Galanin,[99] who calculated that when the electronic transition dipoles of two molecules are randomly oriented the emission anisotropy after a single energy transfer event is close to 0, when the absorption and emission dipoles are parallel and the probes do not rotate. Also, in the case of randomly oriented chromophores undergoing efficient energy transfer, the acceptor steady-state anisotropy is expected to be close to 0.[100]

2. *The orientational distribution of the probes is random.*

3. *The distance of closest approach (R_e) between donor and acceptor is less than the Förster critical distance (R_0).*

The efficiency of transfer can be calculated from the expression for the decay of the intensity parallel and perpendicular to the excitation direction[101]:

$$I(t)_{\text{par}} = \left(\frac{I_0}{3}\right)\left[1 + r_{01}(1 + e^{-Kt}) + r_{02}(1 - e^{-Kt})\right]e^{-\Gamma t} \tag{27}$$

$$I(t)_{\text{perp}} = \left(\frac{I_0}{3}\right)\left[1 + \frac{r_{01}(1 + e^{-Kt})}{2} - \frac{r_{02}(1 - e^{-Kt})}{2}\right]e^{-\Gamma t} \tag{28}$$

[97] C. E. MacPhee, G. J. Howlett, W. H. Sawyer, and A. H. Clayton, *Biochemistry* **38,** 10878 (1999).

[98] P. K. Wobler and B. S. Hudson, *Biophys. J.* **28,** 197 (1979).

[99] V. M. Agranovich and M. D. Galanin, "Electronic Excitation Energy Transfer in Condensed Matter." North-Holland Publishing, New York, 1982.

[100] M. N. Berberan-Santos and B. Valeur, *J. Chem. Phys.* **95,** 8048 (1991).

[101] B. D. Hamman, A. V. Oleinikov, G. G. Jokhadze, R. R. Traut, and D. M. Jameson, *Biochemistry* **35,** 16680 (1996).

where I_0 is the initial intensity, r_{01} and r_{02} are, respectively, the anisotropy decays of the donors and acceptors only, Γ is the fluorescence decay rate, and K is the rate of transfer between donor and acceptor. On integration, and assuming that the rate of back transfer is equal to the rate of forward transfer, a steady-state expression for the efficiency of transfer E is obtained by

$$E = \frac{2(r_{01} - \langle r \rangle)}{r_{01}} \tag{29}$$

where $\langle r \rangle$ is the observed anisotropy (assuming $\langle \kappa^2 \rangle = 2/3$).

Using the Wobler and Hudson equation[98]

$$E = 1 - \left(A_1 \exp^{-k_1 c} + A_2 \exp^{-k_2 c}\right) \tag{30}$$

where A_1, A_2, k_1, and k_2 are constants that depend on the ratio Re/R_0.[98] MacPhee *et al.*[97] showed that the data obtained for their peptide could not be fitted to values of energy transfer expected from fluorophores randomly distributed and oriented on a planar surface. Therefore, they concluded that the high transfer efficiencies they observed were the result of self-association of the peptides on the lipid surface.

Evaluation of Number of Subunits in Oligomer

Runnels and Scarlata[102] described general equations to calculate the expected anisotropy for complexes composed of varying numbers of labeled subunits and applied them to study the oligomerization of the Gag and matrix domains of human immunodeficiency virus type 1 (HIV-1).[103] In the simplest case in which the distances between the fluorophores in the cluster are equal, there is no change in the lifetime of the individual fluorophores, and the anisotropy following a single transfer event is equal to 0, the anisotropy for N molecules (r_ν) can be calculated as

$$r_N = r_1\left(\frac{1 + F\tau}{1 + NF\tau}\right) \tag{31}$$

with the Förster transfer rate, F, assuming that the rates of forward and back transfer are equal ($F = F_{jk} = F_{kj}$):

$$F = \frac{1}{\tau}\left(\frac{R_0}{R}\right)^6 \tag{32}$$

The authors demonstrated that it is possible to determine the number of subunits in a cluster for values of $R/R_0 < 0.8$ (R being the distance separating the centers of the donor and acceptor fluorophores). Blackman *et al.*,[104] on the other hand,

[102] L. W. Runnels and S. F. Scarlata, *Biophys. J.* **69,** 1569 (1995).
[103] S. Scarlata, L. S. Ehrlich, and C. A. Carter, *J. Mol. Biol.* **277,** 161 (1998).
[104] S. M. Blackman, D. W. Piston, and A. H. Beth, *Biophys. J.* **75,** 1117 (1998).

used a Monte Carlo numerical approach to study the oligomeric state of erythrocyte anion-exchange protein (band 3) and showed that the anisotropy decay was consistent with a dimeric and/or tetrameric protein.

Distance Estimation by Homotransfer

Using Eq. (29) and Förster's equation,

$$E = \frac{R_0^6}{(R_0^6 + R^6)} \tag{33}$$

relating the efficiency of transfer E to the critical distance R_0 and R, the distance between the centers of the donor and acceptor fluorophores,[83,101] Hamman *et al.* used homo-FRET to study the separation between subunit domains of the dimeric ribosomal stalk protein L7/L12. Using cysteine mutations, placed by site-directed mutagenesis and labeled with fluorescein, they demonstrated that the C-terminal domains of the protein are, on average, significantly separated, contrary to the model proposed from the crystal structure of the C-terminal domain of the protein.[105] These homo-FRET studies also demonstrated rapid and facile subunit exchange between populations of L7/L12 dimers at concentrations significantly above the dimer/monomer dissociation constants.

It is interesting to note that distances between fluorophores can also be calculated from Eqs. (31) and (32) when the number N of fluorophores is known and for R/R_0 values <0.8 and <1.8. When the distance between two fluorophores is determined as a function of the anisotropy, using both methods [i.e., using Eqs. (29) and (33) or Eqs. (31) and (32)] and the results are compared (Fig. 12), the equations used by Hamman *et al.*[101] will give a slightly smaller distance between the fluorophores than the equations of Runnels and Scarlata.[102] Also, for short distances, when the energy transfer is maximum, and the rates of forward and back transfer are equal, the lowest value for the anisotropy between two fluorophores using both methods will be one-half that of the anisotropy without transfer.

Homotransfer in Vivo

Using a fusion protein between the herpes simplex virus thymidine kinase and the green fluorescent protein (GFP), Gautier *et al.*[106] demonstrated the presence of homotransfer within aggregates that formed in cells transfected with the

[105] M. Leijonmarck and A. Liljas, *J. Mol. Biol.* **195,** 555 (1987).

[106] I. Gautier, M. Tramier, C. Durieux, J. Coppey, R. B. Pansu, J. C. Nicolas, K. Kemnitz, and M. Coppey-Moisan, *Biophys. J.* **80,** 3000 (2001).

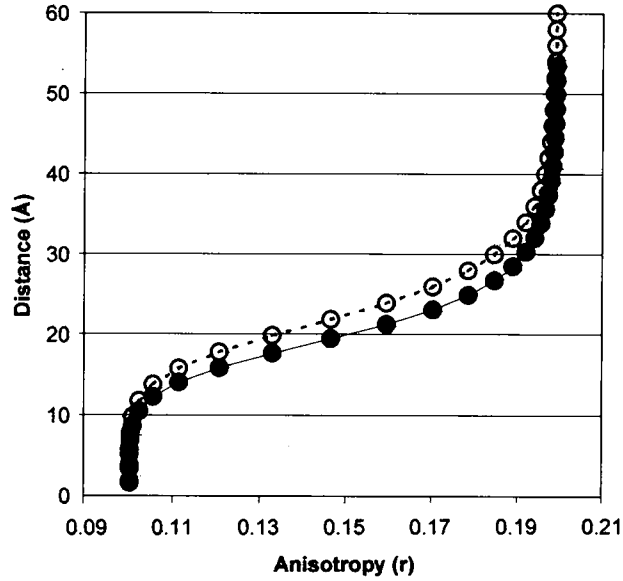

FIG. 12. Distance between two fluorophores calculated from anisotropy after FRET. Open circles represent the results obtained with Eqs. (31) and (32). Solid circles represent the results obtained with Eqs. (29) and (33). The limiting anisotropy was set to 0.2 and the Förster critical distance R_0 was 20 Å.

fusion protein. These researchers uses the equation described by Tanaka and Mataga[107]:

$$r(t) = \frac{3}{20}(2\cos^2\delta - \cos^2\theta_{ij} - \cos^2\theta_{ji})e^{-2\omega t} + \frac{1}{20}(6\cos^2\delta + 3\cos^2\theta_{ij} + 3\cos^2\theta_{ji} - 4) \tag{34}$$

with

$$\omega = \frac{3}{2}\langle\kappa^2\rangle\left(\frac{R_0}{R}\right)^6\tau^{-1} \tag{35}$$

where δ is the intramolecular angle between the absorption and emission transition moments, and θ_{ij} and θ_{ij} are the static mutual orientations of the transition moments of absorption to state i and of emission from state j, and between those of absorption to state j and emission from state i, respectively. Taking into account that (1) in GFP the emission and absorption dipole moments are parallel,[108]

[107] F. Tanaka and N. Mataga, *Photochem. Photobiol.* **29,** 1091 (1979).
[108] A. Volkmer, V. Subramaniam, D. J. Birch, and T. M. Jovin, *Biophys. J.* **78,** 1589 (2000).

(2) rotation of the protein dimer during the fluorescence lifetime is negligible, (3) there is no reorientation of the transition moment during the fluorescence lifetime because the chromophore of GFP is rigidly fixed inside the barrel, and (4) it was likely that the orientation of GFP chromophores was symmetrical within the dimer, Gautier *et al.*[106] calculated, for a dimer, the mutual orientation between the two chromophores and the upper limit of the distance separating the two chromophores.

Failure of Homotransfer on Excitation at Long-Wave Edge of Absorption Spectrum: Red Edge Effect

In 1960, in a study of homotransfer in solutions of tyrosine, tryptophan, and other compounds, Weber showed that concentrated solutions of indole in propylene glycol at $-70°$ did not show significant depolarization when excited at wavelengths longer than 305 nm, whereas depolarization was evident on excitation between 240 and 300 nm.[85] The ratio of the polarization on excitation at 305 and 270 nm (p_{305}/p_{270}), which varies from 1.4 to 1.7 in the simple indole derivatives, was found to be greater than 2 in 9 of the 10 tryptophan-containing proteins studied.[90] A similar observation showing the dependence of energy transfer on the wavelength of the exciting light was reported for 1-anilino-8-naphthalene sulfonate in propylene glycol at $-70°$ or when adsorbed to bovine serum albumin in aqueous solution.[109] In 1970, Weber and Shinitzky[86] studied this effect in more detail and found that in the many aromatic fluorophores they examined (including fluorescein, indole, etc.), unlike a few nonaromatic fluorophores (such as the antibiotic filipin, biacetyl, 4-hydro-*N*-methylnicotinamide, and *N*-butyltriazoline dione), transfer was much decreased or undetectable on excitation at the red edge of the absorption spectrum. More recently, Helms *et al.*[110] made use of homo-FRET and the red edge effect to demonstrate proximity between specific tryptophan residues in a multitryptophan protein. The red-edge drop in energy transfer efficiency (named Weber's red edge effect by Eisinger *et al.*[111]) is characteristic of homo-FRET and is not observed in the case of heterotransfer.[86,111] Berberan-Santos *et al.*[112] have proposed that the lack of energy transfer at the red edge is due to inhomogeneous spectral broadening and the resulting directed energy transfer. The absorption and emission spectrum can be represented as composed of a distribution of spectra corresponding to different fluorophore–solvent configurations. By exciting at the red edge, a subpopulation of fluorophores having a "red" spectrum can be preferentially excited over a subpopulation having a "blue" spectrum. Because the efficiency

[109] S. R. Anderson and G. Weber, *Biochemistry* **8,** 371 (1969).

[110] M. K. Helms, T. L. Hazlett, H. Mizuguchi, C. A. Hasemann, K. Uyeda, and D. M. Jameson, *Biochemistry* **37,** 14057 (1998).

[111] J. Eisinger, A. A. Lamola, J. W. Longworth, and W. B. Gratzer, *Nature (London)* **226,** 113 (1970).

[112] M. N. Berberan-Santos, J. Pouget, and B. Valeur, *J. Phys. Chem.* **97,** 11376 (1993).

of transfer is related to the spectral overlap between the emission spectrum of the donor and the absorption spectrum of the acceptor, the probability of transfer from a "blue" subpopulation to a "red" one is higher than the probability of transfer from a red subpopulation to a blue one. Therefore, on red edge excitation, as the excitation wavelength increases beyond the absorption maximum, the probability of energy transfer from the directly excited chomophore (red subpopulation) decreases because the proportion of the blue subpopulation to which transfer is weak or impossible drastically increases, resulting in the failure of energy transfer. An excellent discussion of red edge effects is given by Valeur.[7]

Summary

We hope that we have conveyed information of interest and value to present and future fluorescence practitioners. Those readers with a sustaining interest in this topic may wish to consult more comprehensive sources such as *Molecular Fluorescence: Principles and Applications,* an excellent text by Valeur,[7] or *Principles of Fluorescence Spectroscopy* by Lakowicz.[24] Many specialized fluorescence topics are covered in the series *Topics in Fluorescence Spectroscopy* (Volumes 1–6), and several volumes of *Methods in Enzymology* (e.g., Volumes 246 and 278) have dealt with issues in fluorescence spectroscopy. Proceedings from the International Conference on Methods and Applications of Fluorescence Spectroscopy, 1997 (MAFS 97)[113] and MAFS 98 (in press) also present fluorescence work on many different topics in biological and chemical fields. The *Molecular Probes Handbook* and web site (www.probes.com) are also rich sources of useful information. Finally, any reader with a question or seeking advice on some topic related to fluorescence is welcome to e-mail D.M.J. at djameson@hawaii.edu.

Acknowledgments

The authors wish to acknowledge support from the National Science Foundation (MCB9808427) and the American Heart Association (9950020N and 0151578Z). They also wish to sincerely thank Gerard Marriott, the long-suffering editor of this volume, for his vast patience.

[113] B. Valeur and J.-C. Brochon, eds., "New Trends in Fluorescence Spectroscopy." Springer-Verlag, Heidelberg, Germany, 2001.